CONFIDENTIAL

Copy 103
RM E55D15

RESEARCH MEMORANDUM

EXPERIMENTAL INVESTIGATION OF DIRECT CONTROL OF DIFFUSER PRESSURE ON 16-INCH RAM-JET ENGINE

By William R. Dunbar, George Vasu, and Herbert G. Hurrell

Lewis Flight Propulsion Laboratory
Cleveland, Ohio

CLASSIFIED DOCUMENT

NATIONAL ADVISORY COMMITTEE FOR AERONAUTICS

WASHINGTON
June 20, 1955

CONFIDENTIAL

NATIONAL ADVISORY COMMITTEE FOR AERONAUTICS

RESEARCH MEMORANDUM

EXPERIMENTAL INVESTIGATION OF DIRECT CONTROL OF DIFFUSER PRESSURE ON 16-INCH RAM-JET ENGINE

By William R. Dunbar, George Vasu, and Herbert G. Hurrell

SUMMARY

The results of an experimental investigation of the steady-state and dynamic performance characteristics of closed-loop control of a ram-jet engine by direct control of diffuser pressure are presented. The investigation was conducted on a 16-inch-diameter ram-jet engine over the range of Mach numbers from 1.5 to 1.99.

The scheduled performance was satisfactorily maintained for operation over the range of Mach numbers and during changes in exhaust-nozzle area of 20 percent and changes of angle of attack up to 10°.

Transient response times approaching the system dead time of 0.035 second were obtained for controller constants near the system stability limits, and the approximate limits of controller constants which would provide a response time of 0.1 second with less than 10 percent overshoot were obtained. Stability limits of the system predicted from engine dynamic characteristics were verified experimentally.

INTRODUCTION

Effective utilization of the ram-jet engine as a propulsion system for supersonic flight is dependent, to a great extent, on the development of suitable engine-control systems. The control system must, in general, be capable of maintaining desired engine performance throughout the flight plan and minimizing departures from desired performance due to transient disturbances within the system or in flight conditions. Analyses (refs. 1 and 2) have indicated some ram-jet engine parameters suitable for control purposes and techniques for their application in control loops.

In order to investigate ram-jet engine dynamics and to ascertain the practicability of several control techniques, including optimalizing, shock positioning, and diffuser-pressure control techniques, an

experimental investigation was conducted on a full-scale ram-jet engine in the 8- by 6-foot supersonic wind tunnel of the NACA Lewis laboratory. The preliminary results of the investigation are reported in reference 3.

The results of the investigation of direct control of diffuser pressure are presented herein. In this control, the diffuser-exit total pressure was maintained as a function of free-stream Mach number, altitude, and angle of attack in accordance with a preset schedule. The investigation of the controlled system included the steady-state operation at Mach numbers from 1.5 to 1.99 and the dynamic performance for disturbances in fuel flow, angle of attack, and exhaust nozzle area.

The primary objectives of the investigation were: (1) to determine if the control technique would perform satisfactorily when applied to an actual engine control system; (2) to determine how accurately the desired performance could be maintained, and (3) to investigate the dynamic response of the system as affected by different magnitudes and types of disturbances and variations in controller constants.

A secondary objective of the investigation was that of observing two other engine parameters, diffuser-exit static pressure and diffuser-exit Mach number, with respect to their suitability in control loops. The results are presented in a discussion of experimental curves showing the steady-state and transient performance of the controlled system and oscillographic records of typical transients.

DESCRIPTION OF CONTROL

Diffuser-Pressure-Control Concept

The concept of the diffuser pressure control is based on the interrelation of diffuser and engine performance as shown in the performance map of figure 1. In this figure the diffuser pressure ratio, the thrust coefficient, and the specific fuel consumption are shown as functions of engine total-temperature ratio. (The diffuser-pressure-ratio characteristics are averaged curves obtained from data presented in ref. 3. The thrust and specific-fuel-consumption characteristics were obtained from data presented in ref. 4 adjusted from exhaust-nozzle area of 0.990 sq ft to 0.960 sq ft.) All symbols used in the report are defined in appendix A. As may be seen in figure 1, a specified level of thrust at a particular flight condition requires a unique value of diffuser pressure ratio, providing operation is limited to the supercritical region of diffuser operation. As an example, if a thrust level equal to a thrust coefficient of 0.55 is desired at a Mach number of 1.98 and zero angle of attack, the diffuser must be operated at a pressure ratio of 6.4.

The versatility of this type of control is apparent since any desired level of thrust over the entire supercritical operating range of the engine may be obtained by setting the appropriate diffuser pressure as a function of flight conditions. The exclusion of the critical and subcritical operating regions will be discussed later.

In a fixed-geometry ram-jet engine the only independent variable that may be manipulated to achieve a desired mode of operation is the fuel flow. The variation of diffuser pressure ratio with fuel flow for the engine tested is shown in figure 2. The curves presented are averaged curves of data taken in the investigation reported in reference 3.

Fuel flow can be scheduled directly in order to obtain a desired engine operating condition, but because of such problems as the limitations of the accuracy of fuel metering, variation in fuel properties, and variations in combustion efficiency there is no assurance of obtaining the desired performance. By direct closed-loop control of diffuser pressure, however, these problems are not reflected in control operation in steady state.

The sequence of control operation may be seen with respect to the assumed control point shown in figure 2. The pressure ratio shown of 6.4 at a Mach number of 1.98 and zero angle of attack represents the desired or set value. The actual magnitude of P_x/p_0 is measured at the engine and compared with the set value in the manner shown in the simplified block diagram of figure 3. The difference between the actual and set values of diffuser pressure ratio is the error signal ϵ. The control and fuel servo respond to the error signal by increasing or decreasing the fuel flow as required to bring the error signal to zero.

The technique of control has certain inherent limitations, which may be shown by figure 2. Any disturbance sufficiently large to cause the engine to operate subcritically at pressure ratios less than the set value of 6.4 would give an incorrect error signal which would tend to drive the engine further subcritical, resulting in either engine failure or combustion blow-out. This limitation may be overcome by use of a suitable limiting device to prevent continued subcritical operation. This characteristic also makes the control inherently unstable for operation at peak pressure ratio without a suitable limiting device, since the control could not distinguish any difference between disturbances in either supercritical or subcritical directions.

Description of System Tested

Reference input. - The reference input represents the desired diffuser pressure as determined by the flight plan. In the event of

piloted applications the reference input could be the pilot's signal for a desired thrust level, since the relation of thrust coefficient to diffuser pressure is nominally linear for fixed flight conditions. In general, however, the reference input must be obtained as a function of altitude, flight Mach number, and angle of attack. There are many possible systems for providing such an input depending on the operating requirements of a particular application. The system employed during the test program inherently provided the required compensation for the effects of altitude pressure and was indicative of the peak diffuser pressure obtainable as a function of flight Mach number and angle of attack.

The indication of the maximum pressure capability of the diffuser was obtained by means of a total-pressure tube located above the surface of an auxiliary cone, similar to the engine cone, so that, in the Mach number range of the tests, it was always behind the conical shock wave. Details of the installation are given in the Instrumentation section. The pressure indication thus obtained is independent of engine operating conditions and is directly dependent on flight conditions. For a single oblique-shock diffuser, as on the engine tested, the pressure obtained is indicative of the maximum diffuser pressure obtainable, neglecting subsonic-diffuser losses, since both are pressures behind oblique shocks of the same strength and normal shocks of approximately the same strength.

The choice of a reference input made herein is only one of a number of possible choices and was selected because of its ready availability and the simplification it permitted in the control, as described in the following section.

Schedule of reference input. - The variation of the reference pressure ratio P'_{ac}/p_0 and the maximum average diffuser pressure ratio $P_{x,max}/p_0$ with free-stream Mach number and angle of attack is shown in figure 4. These data are presented again in figure 5 to show the variation of $P_{x,max}/P'_{ac}$ with free-stream Mach number for various angles of attack. For angles of attack of 5° or less, $P_{x,max}/P'_{ac}$ is approximately constant over the range of Mach numbers investigated. At an angle of attack of 10° the ratio drops consistently from 0.96 at a Mach number of 1.5 to 0.875 at a Mach number of 1.98. The essentially constant $P_{x,max}/p_0/P'_{ac}/p_0$ at low angles of attack permitted the use of a simple and easily obtainable schedule for test purposes.

The schedule used set P_x as a fixed percentage of P'_{ac} as indicated by the dashed lines of figure 5. The 0.9 schedule provided for operation at approximately 96 percent of peak diffuser pressure over the range of Mach numbers at zero angle of attack. The 0.85 schedule

sets approximately 91 percent of peak pressure for the same range of conditions and in addition permits operation at a Mach number of 1.98 and an angle of attack of 10° at approximately 97 percent of peak pressure.

Limits. - In order to prevent instability of the control due to subcritical operation, two types of limits were used. The first was a maximum fuel-flow limit which, because of the special conditions encountered in the operation of the wind tunnel, could be set as a fixed value. The variation of altitude with Mach number encountered in tunnel operation was such that for supercritical operation the mass flow through the engine varied only slightly (approximately 10 percent) over the range of test conditions. Thus, as may be seen in figure 2, it is possible to select a fixed value of fuel flow that would provide a suitable limit for operation of the engine for all flight conditions shown. This type of limit obviously requires adjustment for Mach number and altitude for use in actual flight and is affected by variations in combustion efficiency.

The second limit, a shock-location sensing limit, was an application of a separate control technique reported in reference 3. As used herein, in a limiting device, the system operated in the following manner. The difference in static pressure Δp_L existing between the diffuser inlet and the cone surface near the tip of the spike was measured with a differential pressure transducer. For diffuser operation with no external normal shock, this differential pressure is nominally zero. For operation of the diffuser with an external normal shock, however, the static pressure at the inlet is larger than the cone-surface pressure as a result of the static-pressure rise across the shock. The differential pressure is then indicative of the presence of a normal shock external to the diffuser and was used to override the diffuser pressure control and prevent continued subcritical operation.

The diffuser used had internal contraction. Because of its characteristics, operation at Mach numbers below approximately 1.79 always results in an external normal shock or bow wave. The bow wave does not necessarily preclude the use of the differential pressure as an indication of subcritical operation, since the diffuser-inlet pressure does increase as subcritical operation is reached, although the transition is not as abrupt as is the case for operation at higher Mach numbers. However, additional complexity in the limit loop of the control would be required in order to provide the necessary compensation for the effects of the bow wave.

To avoid this complexity, operation of the engine with this type of limit was restricted to Mach numbers of 1.79 or greater, where the available data indicated that the limit could be utilized with a minimum amount of adjustment for Mach number, altitude, and angle of attack.

In the actual test the limit signal was adjusted to provide zero output at a Mach number of 1.79 and zero angle of attack for supercritical operation, and was not further adjusted for the remainder of the tests.

Control-loop components. - In figures 6(a) and (b) are shown the block diagram and connection diagram, respectively, of the control system used for the tests, including both types of limits, only one of which was connected at a time. In normal operation with the shock-position limiter the voltage $V_{\Delta p_L}$, obtained from Δp_L, is zero and does not affect control operation. The reference value $V_{P'_{ac}}$ is obtained from the pressure P'_{ac} multiplied by a fixed percentage, corresponding to the schedule desired. The control variable P_x is sensed at the diffuser exit and the amplified signal V_{P_x} is compared with the set value $V_{P'_{ac}}$. The difference between the set and actual values ε is acted on by the control, which has proportional-plus-integral action. The control then drives the fuel servo, which varies the fuel flow as required in order to bring the error signal to zero.

The control-loop component sensitivities are as follows:

Fuel servo, lb/hr/volt	278
Engine, (lb/sq ft)/(lb/hr)	0.317 to 0.532 (depending on operating point)
Pressure sensor and carrier amplifier, mv/lb/sq ft	0.622
Control	Variable gain and integrator rate depending on constants set in computer

The frequency-response characteristics of the control-loop components are shown in figures 7(a) and (b) for the fuel servo, W_f/V_i; for the engine, sensor, and amplifier, V_{P_x}/W_f; for the over-all characteristic excluding the control computer V_{P_x}/V_i; and for the control computer for a typical set of constants. The effect of the sensor and amplifier on the curve of V_{P_x}/W_f is negligible at the frequencies shown. Actual curves for sensors and amplifiers are given in appendix B.

APPARATUS AND INSTRUMENTATION

Engine and Installation

The 16-inch-diameter ram-jet engine used in this test program is shown in the cutaway drawing of figure 8. The diffuser was a single-oblique-shock, internal-contraction type with a 25° half-angle conical

spike. The engine was equipped with a can-type combustor and a conical exhaust nozzle with an exit area of 0.960 square feet, equal to 0.69 of the combustion-chamber area. The fuel-injection system in the engine comprised primary and secondary manifolds located 17 inches upstream of the combustor can. A pilot burner was included in the system and was located just forward of the can. The fuel used was MIL-F-5624B, grade JP-4, amendment 1.

The installation of the engine in the 8- by 6-foot supersonic wind tunnel is shown in figure 9. The engine was supported by a strut which was pivoted to permit a variation of angle of attack from 0° to 10°. Reductions in nozzle-exit area of as much as 20.3 percent of the maximum value could be obtained by use of a movable water-cooled plug. A detailed description of the engine and its steady-state performance is given in reference 4.

Control Equipment

For the present tests the fuel flow to the pilot burner and primary fuel manifold was set at a fixed value and all adjustments to fuel flow were made in the secondary fuel manifold by means of a fuel servo. The fuel-servo system contained an electrohydraulic servo system which positioned a throttle in a specially designed fuel-metering valve in response to an input voltage signal. The fuel-metering valve incorporated a differential relief valve which maintained a constant pressure differential across a metering orifice. Since the metering area was a linear function of throttle position, the fuel flow was also a linear function of throttle position and of the input voltage to the fuel servo. This type of fuel system is described in detail in reference 5.

The necessary control computations were performed with an electronic differential analyzer comprising racks 4 and 5 of figure 10. The computer utilizes high-gain d-c operational amplifiers with associated plug-in input and feedback impedances to perform its functions. The output of the control computer goes to the fuel-control chassis located in rack 3. Racks 1, 2, and 6 contain accessory equipment and the recording oscillographs and carrier amplifiers.

Instrumentation

The engine variables used for control purposes were sensed with pressure transducers of the variable reluctance type, having high natural frequencies. The connecting tubing to the various pressure taps was kept to a minimum and sized to give good response. The over-all results were such that errors introduced by the pressure sensors and tubing were negligible in the range of frequencies of principal interest.

The diffuser total pressure P_x was sensed at the diffuser exit by means of a single total-pressure tube, which was selected from previous data as indicative of the average pressure. The limit signal Δp_L was the static-pressure differential of a tap located on the horizontal centerline of the innerbody in the plane of the cowl lip and a tap 1 inch downstream of the tip of the spike, also on the horizontal centerline. The reference pressure P'_{ac} was measured by means of four manifolded total-pressure tubes mounted on a small model of the engine cone as shown in figure 11. The auxiliary cone was located so that in the Mach number range of the tests there would be no chance of interference with the engine shock pattern. The total-pressure tubes on the cone were located above the cone surface so that, for the Mach number range encountered, they were always behind the conical shock. The tubes were oriented on axes parallel to the horizontal and vertical centerline axes of the engine. Further details on other instrumentation installations are given in appendix B.

TEST PROCEDURE

Steady-State Operation

The steady-state performance of the control system was investigated by operating the engine with the fixed fuel-flow limit set at 3475 pounds per hour on the 0.9 P'_{ac} schedule at zero angle of attack from Mach numbers of 1.5 to 1.99 at altitudes of 26,000 to 37,000 feet, respectively. With the shock-position limit the engine was operated on the 0.85 P'_{ac} schedule at zero angle of attack from Mach numbers of 1.8 to 1.99 at corresponding altitudes of 33,000 to 37,000 feet.

Transient Operation

The behavior of the engine and control system during transients was investigated by means of the following series of disturbances: (1) Step disturbances of fixed magnitude imposed on the input voltage to the fuel servo V_i for various control settings at fixed flight conditions; (2) step disturbances of varying magnitude in V_i with two types of limits for fixed control settings at fixed flight conditions; (3) a variation in exhaust-nozzle area of 20.3 percent with fixed control settings at a single flight condition; and (4) a change in angle of attack from 0° to $+10^\circ$ with fixed control settings at a single flight condition.

RESULTS AND DISCUSSION

Steady-State Performance

The steady-state performance of the controlled engine is discussed primarily with regard to the accuracy with which the control maintained the desired operating condition and the sources of error which were observed, and secondarily with regard to the effects on steady-state operation of the two limits tested.

Operating line. - The operating lines for the control are shown on the performance map of figure 12, for both the 0.9 and 0.85 P'_{ac} schedules. The scheduled operation is shown as the dashed lines, which connect the scheduled values at Mach numbers of 1.5, 1.79, and 1.98. The actual operation achieved is shown as the data points connected by the broken lines. Operation on the 0.9 P'_{ac} schedule resulted in stable performance from a Mach number of 1.5 to 1.90 at diffuser pressure ratios 2 to 3 percent higher than scheduled. At a Mach number of 1.99 the engine was off schedule and operating against the fixed fuel-flow limit.

Operation on the 0.85 P'_{ac} schedule was stable from a Mach number of 1.79 to 1.99 with the pressure ratio again 2 to 3 percent higher than scheduled. Operation at Mach numbers below 1.79 was not attempted with the shock-position limit because of the effects of the bow wave previously discussed.

The actual operating points are also shown on the thrust and specific-fuel-consumption curves to indicate the corresponding engine performance obtained.

Deviation from scheduled performance. - The ratios of the controlled diffuser pressure $P_{x,c}$ and the average diffuser pressure $P_{x,av}$ to the maximum diffuser pressure $P_{x,max}$ are presented in figure 13 as a function of flight Mach number from data obtained during operation with the control. The scheduled diffuser pressure ratios for 0.9 and 0.85 of $P'_{ac}/P_{x,max}$ are shown by the solid lines. The measured values of $P_{x,c}/P_{x,max}$, which are indicated by the open data points, where $P_{x,c}$ is the controlled variable, fall precisely on the schedule curves; therefore, no error can be attributed to the control components. The fact that the average diffuser pressure ratio shown by the solid data points is higher than scheduled is attributed to variation in the relation between the average diffuser pressure $P_{x,av}$ and the controlled diffuser pressure $P_{x,c}$ where the latter was sensed by a single tube.

The reason that the engine went off control at a Mach number of 1.99 on the 0.9 P'_{ac} schedule is clearly indicated by observing the trend of the average pressures as Mach number increases. By extrapolating the curve of the average pressures to a Mach number of 1.99, it is apparent that the control was attempting to set the average pressure at approximately 99.5 percent of the maximum obtainable. Attempting to operate within 0.5 percent of maximum represented an insufficient margin; and, consequently, either the noise level of the engine or a random disturbance caused the diffuser to operate subcritically and resulted in continued operation against the fuel-flow limit.

Effect of limits. - The fixed maximum fuel-flow limit had no adverse effects on steady-state operation, but it must be emphasized that, if this type of limit were used in flight, it would require adjustment as a function of flight conditions and would be affected by any variation in combustion efficiency.

The shock-position limit, however, is independent of variations in combustion efficiency and over the range of Mach numbers tested (1.79 to 1.99) required no adjustment for changes in Mach number or altitude. There was some effect of altitude and Mach number on the limit signal, but for the limited range of the tests the variation could have contributed only approximately 0.5-percent error to the set value of P_x. Over a more extended range of flight conditions, a larger effect might normally occur and some adjustment might be required. For operation below the diffuser starting Mach number of 1.79 for this engine, the effects of the bow wave must be considered in order to prevent adverse effects. The effects of angle of attack on the limit parameter will be discussed in the section Angle-of-attack transient.

Dynamic Performance

The results of the transient tests are presented in order to demonstrate the effect of various controller constants on the dynamic performance of the system and to demonstrate the operation of the system when subjected to various sizes and types of disturbances.

Stability limits. - The effects of controller settings on system stability are presented for two extremes of controller operation: (1) for primarily proportional control action with very slow integrator rate, and (2) for primarily integral action with very low proportional loop gain. The control, however, includes both proportional and integral action at all times. The control transfer function is expressed as $K(1 + 1/\tau S)$, where K is the proportional gain, τ is the integrator time constant in seconds, and S is the complex operator. The loop gains referred to hereinafter are the product of the controller

gain K and the sensitivities of the other control-loop components as determined from their steady-state characteristics. The effects of various controller settings were measured in terms of the amplitude and frequency of the oscillations observed in the fuel flow at each condition. The amplitude was taken as one-half the peak-to-peak value of the maximum fluctuations encountered. The frequency was measured only if a single frequency or predominant band of frequencies was clearly discernible in the fluctuations; otherwise, it is indicated as zero. With no control action there is a certain amount of fluctuation in the fuel flow, originating in the pump, manifold, and so forth, which is indicated as the "noise level" of the system.

The effects of varying the loop gain with a constant low integrator rate are shown in figure 14. As the loop gain is increased, for values less than 1.52, the fuel-flow oscillations gradually increase to approximately 350 pounds per hour but remain irregular in amplitude and frequency. The frequency points, shown connected by vertical lines, indicate the range of frequencies observed at these conditions. The nature of the oscillations encountered at loop gains less than 1.52 is shown in the oscillogram of figure 15 for a loop gain of 1.36. Note that the fuel-flow oscillations observed in the trace of secondary-nozzle pressure drop are not sustained or of regular frequency but tend to be damped out. The fluctuations seen in secondary-nozzle pressure drop also appear in the other control-loop variables such as servo input voltage, fuel-valve position, and diffuser-exit total pressure. As the loop gain is increased slightly beyond 1.52, the oscillations become sustained and of regular frequency, as shown in the oscillogram of figure 16 for a loop gain of 1.525. The marked change in the nature of the oscillations is readily apparent by comparison of figures 15 and 16. The oscillations in fuel flow have become quite regular with a single pronounced frequency and are more than twice the amplitude of the maximum oscillation observed in figure 15.

The stability limit, as used herein, is defined as the condition at which sustained, regular oscillations occur. Therefore, the experimental stability limit is set at a loop gain of 1.52, with the frequency of oscillation equal to 12 cps, for the following set of operating conditions: flight Mach number, 1.5; zero angle of attack; 0.9 P'_{ac} schedule; and the integrator time constant τ, 0.05 second. This experimental limit compares closely with the value of loop gain equal to 1.49 at a frequency of 12 cps calculated from the frequency-response curves of figure 7 for the same integrator time constant.

For the second set of control conditions, that is, a constant low loop gain and a variable integrator rate, the effects of varying the integrator time constant are shown in figure 17. With primarily integral control action, as the integrator rate is increased the oscillation

amplitude remains essentially constant at the normal noise level with no regular frequencies discernible up to $1/\tau = 100$ sec^{-1}. At this condition a slight oscillation of 40 pounds per hour at 8 cps was observed. The range over which the integrator rate could be varied was not sufficient to define the stability limit, but the trends shown in figure 17 are consistent with the calculated value of $1/\tau$ equal to 126 sec^{-1} and frequency of oscillation equal to 8 cps for a proportional loop gain of 0.339.

Response characteristics. - The effects of various control settings on the response characteristics of the system were observed for the same extremes of control operation previously discussed, that is, mainly proportional action and mainly integral action. The response characteristics measured were the response time and the percent overshoot for a step disturbance in the input voltage to the fuel servo. The response time as used herein is defined as the time from initiation of a disturbance until 90 percent of the error has been initially corrected. Overshoot is defined as the ratio of the maximum overshoot occurring during the transient to the magnitude of the initial disturbance, expressed in percentage form.

The response characteristic is shown as a function of loop gain in figure 18(a) for a low integrator rate. The stability curves for this same set of conditions are repeated for convenient reference. As the loop gain is increased, the response time decreases rapidly until it is approximately 0.06 second at a loop gain of 1.02. For higher values of loop gain, the response time decreases very slightly and the percent overshoot begins to increase rapidly until the stability limit is reached at a loop gain of 1.52.

The response characteristic as a function of integrator time constant is shown in figure 18(b) for a low loop gain. As in figure 18(a) the corresponding stability characteristic is shown for reference. As the integrator rate is increased, the response time decreases continuously, reaching its smallest value of 0.07 second at the maximum rate obtained of 100 sec^{-1}. Since the stability limit has not been reached, some additional reduction in response time could be expected; however, as indicated by the percent-overshoot curve, the reduction would be obtained with rapidly increasing overshoot.

In order to permit a comparison of the two types of control action, some of the data from figures 14, 17, and 18 have been cross-plotted in figure 19 to show fuel-flow oscillation amplitude and percent overshoot as a function of response time for both types of control action. It is readily apparent from figure 19 that both types of control action result in nearly identical characteristics for response times as low as 0.1 second. Below 0.1 second, the difference in characteristics is not

indicated because of the limited integrator rates tested. However, the proportional action should tend to give somewhat shorter minimum response times since it resulted in a slightly higher frequency of oscillation than the integral action, that is, 12 cps compared with 8 cps. A response time of 0.1 second with overshoot and oscillation amplitude of less than 10 percent and 50 pounds per hour, respectively, may be obtained with either range of settings shown. Since the two sets of curves represent the extremes of control settings, the approximate limits may be specified for this type of response. These limits are: $\tau = 0.02$ second when loop gain = 0.339; and $\tau = 0.05$ second when loop gain = 1.0.

The difference in response in step disturbances up and down in fuel flow is due to the variation of the engine sensitivity as the operating point shifts during the transient and to the effect of a limited error signal available for a step up. Typical transients of a step up and a step down for the same set of conditions are shown in the oscillograms of figure 20. Some interesting characteristics visible in both figures are: From initiation of the transient at point a on the servo-input-voltage trace until the secondary-nozzle pressure drop responds at point b, there is a dead time of approximately 0.01 second. A further dead time of 0.025 second is evident from point b to point c, where the diffuser-exit total pressure responds. The total system dead time of 0.035 second appears in the servo-input-voltage trace from point a to d, after which corrective action commences. The system dead time of 0.035 second is indicative of the absolute minimum response time for this control system regardless of the variations in control settings attempted. It is interesting to note that the range of integrator time constants previously indicated as suitable are of the same order of magnitude as the system dead time.

Effects of disturbance magnitude. - The response characteristic for various sizes of disturbances was primarily a function of the type of limit employed. In figure 21 an oscillogram is shown of a step disturbance in fuel-servo-input voltage large enough to cause operation of the fixed fuel-flow limit. The time from point a to b on the fuel-valve-position trace is mainly the time required for the control to integrate off the limit. The engine is operating subcritically during a part of the transient, as seen on the diffuser-exit total-pressure trace from point c to d. A hysteresis effect on the diffuser is observable in that the peak pressure occurring at point d is lower than that at point c. The hysteresis may also be seen in the error-signal trace.

The transient is plotted in figure 22 with respect to the steady-state characteristics for Mach numbers of 1.5 and 1.79. The transient commences at the point marked 0 second and follows the path indicated by the arrows. The period of subcritical operation previously observed

from the pressure trace in the oscillogram lasts from time equal to 0.07 second at point c until 0.26 second at point d. During this period of 0.19 second the diffuser does not show any indication of the instability or "buzz" normally occurring in subcritical operation. The overshoot of the fuel flow beyond the value set by the limit (3475 lb/hr) is due to the dynamics of the fuel system.

The response times and percent overshoot for various magnitudes of disturbances are shown in figure 23. The operating point was such that a step up of greater than approximately 25 percent of the initial fuel flow increased the fuel flow sufficiently to cause operation of the fixed fuel-flow limit. For steps up of greater than 25 percent, the response time and percent overshoot increase in nearly a linear manner, since the control acts as a pure integrator; however, for steps down the response characteristic is essentially independent of magnitude of disturbance.

The operation of the shock-position limit is shown in the oscillogram of figure 24 for a step disturbance of +4 volts in servo input voltage, which is equivalent to a change of +1112 pounds per hour in fuel flow. The sequence of action is as follows: At point a, a disturbance of +4 volts is imposed on the servo input voltage; 0.01 second later (point b), the secondary-nozzle pressure drop responds; 0.025 second later (point c), the diffuser-exit total pressure responds; and the control commences corrective action at point d. The corrective action continues until point e, where the diffuser-exit total pressure has increased to its peak value and the normal shock has moved forward to the cowl lip causing operation of the limit signal (point f). The limit action rapidly reduces the servo input voltage and the fuel flow to a minimum lean value of secondary flow of approximately 400 pounds per hour. At point h the diffuser-exit total pressure has increased to its maximum value on the return path, which is lower than at point e, indicating a hysteresis effect in the diffuser pressure. At point i the shock moves back inside the diffuser and the limit signal returns to zero. At this time (point j), the diffuser-exit total pressure is very nearly at the desired value; however, because of the engine dead time it is still responding to the fuel-flow conditions existing 0.025 second earlier and therefore continues to decrease. This action causes the servo input voltage to begin increasing in order to correct the downward trend; but, because of the dynamics of the fuel system at very low flow, the fuel flow does not respond until point k. As a result, the duration of the lean operating portion of the transient is prolonged for a greater time than the original disturbance into the rich operating region. The severity of the limit action as seen here can be reduced by a more reasonable setting of the gain in the limit loop.

The transient is shown with respect to the steady-state characteristic in figure 25. It should be noted that the diffuser is subcritical

from a time of 0.065 second until 0.10 second, corresponding to points e and h on the oscillogram. During this time there was no evidence of buzz, although the engine was subjected to violent buzzing when subcritically operated in steady state at this Mach number. These data indicate that, with sufficiently fast control action, short periods of subcritical operation may be tolerated without intitiation of buzz.

The response times and percent overshoot for various magnitudes of disturbance are shown in figure 26 for operation with the shock-position limit. For the data shown in this figure, step disturbances up greater than approximately 40 percent of the initial fuel flow were large enough to cause operation of the limit. For step disturbances down of increasing magnitude, the response time and overshoot increase slightly in a nearly linear manner, primarily because of the fuel-system dynamics at low flow. For steps up the response time and overshoot increase slightly until the disturbance is large enough to operate the limit. The response time then decreases to a lower value and remains essentially constant thereafter at approximately 0.057 second. Since the limit reduced the fuel flow to the same lean value whenever it operated, regardless of the magnitude of disturbance, the percent overshoot decreases in a nearly linear fashion as shown.

Exhaust-nozzle area change. - A transient in the exhaust-nozzle area is shown in the oscillogram of figure 27 for operation at a Mach number of 1.99 on the 0.85 P'_{ac} schedule. The area was changed from 0.960 square foot to 0.765 square foot in approximately 0.15 second at a maximum rate of change of 2.4 square feet per second. At constant fuel flow this change of area would result in operation of the engine at a pressure ratio of 6.20 in the extreme subcritical region. With the control action the maximum deviation of diffuser-exit total pressure from the set value was 85 pounds per square foot, or approximately 3 percent. At no time during the transient did the engine operate subcritically.

Since the area transient is relatively slow in starting, the engine dead time cannot be indicated precisely. However, from the time the area begins to change at approximately point a in figure 27, there is an elapsed time of 0.02 to 0.03 second until diffuser-exit total pressure responds at point b and servo input voltage begins corrective action at point c.

Angle-of-attack transient. - A transient in angle of attack is shown in figures 28(a) and (b). The engine was initially operating on the 0.85 P'_{ac} schedule at a Mach number of 1.99 and zero angle of attack. The angle was then increased to 10° in approximately 2.3 seconds as shown in the oscillogram. The control operating point was affected during the transient by several factors, some of which are evident in the transient record. The first of these factors appeared almost immediately after the start of the transient at zero angle of attack and

may be seen as the downward shift of the limit signal, which represents an increase in the pressure indication. This caused the fuel flow to decrease slightly which reduced the diffuser-exit total pressure. The next apparent factor is the decrease in the reference input signal, which commenced at about 3°, which also tends to reduce the set value of diffuser-exit total pressure. A third factor, not visible in the traces, is the shift of the pressure profile in the diffuser which alters the relation of $P_{x,c}$ to $P_{x,av}$. The available data for this operating condition indicate that the ratio of $P_{x,c}/P_{x,av}$ was changed from 0.965 at 0° to 0.993 at 10°. The over-all effect of these factors resulted in stable operation up to 10° at pressure ratios approximately 2.5 percent higher than originally scheduled.

However, when the engine is operated near maximum pressure ratio off control at an angle of attack of 10°, it is normally subject to violent instability, which in previous tests frequently resulted in combustion blow-out. This characteristic instability appears in the operation on control just as the engine reaches an angle of attack of 10°. As shown in figure 28(b) the diffuser-exit total pressure suddenly increases at point a, and at point b the shock moves past the cowl lip and the limit operates. The system recovered from this disturbance and operated for a short time (0.5 sec) in a normal manner. Then the engine again attempted to operate subcritically and the limit functioned at point c. This type of operation continued in a cyclic manner, with the limit preventing continued subcritical operation and the subsequent instability normally encountered.

Improvement and Application of Control Technique

The results which are discussed in the preceding sections are dependent to a great extent on the characteristics, both static and dynamic, of the particular engine parameter selected for use in the control. With the objective of possible improvement of the control, two additional engine variables are discussed herein with regard to their suitability as control parameters. In addition, since the ultimate usefulness of the control technique presented in this report depends on its ability to satisfy the requirements of a flight plan, a possible application is presented.

Control parameters. - The performance maps for two other engine variables, diffuser static pressure and diffuser-exit Mach number, are shown in figures 29 and 30, respectively. The diffuser static-pressure characteristic is similar to that of the total pressure and is amenable to similar types of schedules and controls. It is also apparent that control of static pressure requires the same precautions with respect to subcritical operation. The diffuser-exit Mach number however, is an

entirely different type of variable as shown in figure 30. The data for all flight Mach numbers and angles of attack tested may be represented, within the accuracy of measurement, by a single general curve as a function of engine total-temperature ratio. The actual range of diffuser-exit Mach number is fairly limited (0.185 to 0.40) for the entire operating range of engine temperature ratios.

As a comparison of the parameters, the variation of maximum pressure ratio, both total and static, and the corresponding diffuser-exit Mach number are shown in figure 31 as a function of flight Mach number and angle of attack. As mentioned previously, the static-pressure variation is similar to that of the total pressure for the range of conditions shown. The diffuser-exit Mach number, however, is essentially constant for this engine for operation at maximum pressure ratio over the range of flight conditions as observed. This characteristic suggests the possibility of a simple control schedule for operation at maximum pressure ratio by holding the diffuser-exit Mach number constant.

In addition to the types of schedules possible with various control parameters, consideration must be given to the accuracy with which they may be measured. The comparative accuracy of measurement of the three variables discussed is indicated in figure 32 for a series of data points obtained during operation on 0.9 P'_{ac} schedule control. The indicated values of $P_{x,c}$, as previously observed, are within 3.5 percent of $P_{x,av}$ with a total variation of less than 2 percent over the range of flight Mach numbers shown. The indicated values of $p_{x,c}$ are within 0.4 percent of $p_{x,av}$ for the range of conditions. The values of $M_{x,c}$, obtained from $p_{x,c}/P_{x,c}$, however, are only within 40 percent of $M_{x,av}$, obtained from $p_{x,av}/P_{x,av}$, with a total variation of 22 percent. The excessive variation in M_x is indicative of the inherent difficulty of measuring Mach number in this range (0.15 to 0.35) by use of the ratio of static to total pressure. Any error in either pressure is amplified approximately 12.5 times in determining M_x by this method. By use of the ratio $(P - p)/p$, the accuracy may be improved by roughly a factor of three, but Mach number remains the most difficult of the three variables to measure precisely.

Of the three variables mentioned, the static pressure appears to be the most desirable for use in a control for the following basic reasons: (1) Measurements are generally more accurate because the pressure profile is more uniform; (2) there is less noise in the static-pressure signal than in the total, which contributes to better control action; and (3) the better dynamic characteristics of the static pressure, such as a shorter dead time, observed during the investigation,

[redacted]

not only speed up control action directly by responding more rapidly to changes but also tend to increase the frequency of instability by causing less phase shift in the frequency response characteristics.

Application of control. - As an indication of a possible application of the control technique discussed herein, a schedule for engine operation to provide acceleration to cruise Mach number and operation at fixed Mach number thereafter is presented. The thrust coefficient of the engine tested as a function of flight Mach number for various values of diffuser pressure ratio is shown in figure 33. Superimposed on this set of characteristics is an assumed airframe-drag-coefficient curve, with the desired cruise speed at a Mach number of 2.0. The entire operation may be scheduled by setting a single value of pressure ratio as the reference input and operating in conjunction with an appropriate limit, such as the shock-position limit tested. The vehicle would be accelerated by a booster to a Mach number of 1.7, at which point the controlled engine would take over and operate as follows. Since the set pressure ratio of 6.0 cannot be realized by supercritical engine operation at a Mach number of 1.7, the engine would operate at the limit. In addition, since the thrust obtained for critical operation at this Mach number is greater than the drag, the vehicle will accelerate and will continue to accelerate in this manner until reaching a Mach number of 1.9. At this speed, the desired pressure ratio of 6.0 may be obtained with supercritical operation; the engine therefore ceases operating at the limit and operates at the scheduled pressure ratio. Since the thrust is still larger than the drag, the vehicle continues to accelerate until the desired cruise condition is reached. At this point, the control is inherently stable with respect to flight Mach number, since a further increase in speed results in less thrust than drag causing the vehicle to decelerate and a decrease in speed from the set value results in more thrust than drag causing the vehicle to accelerate. Thus, operation of the engine at constant pressure ratio provides a simple and basically stable system to provide for operation at constant Mach number.

CONCLUSIONS

The following results and conclusions were obtained from a supersonic wind tunnel investigation of closed-loop control of a ram-jet engine.

Control of ram-jet performance by direct control of diffuser pressure appears to offer a practicable control technique capable of maintaining desired performance in steady state and of minimizing departures from desired performance due to transient disturbances.

The controlled variable was maintained precisely at the set value, within the limits of measurement, over the range of free-stream Mach

numbers from 1.5 to 1.99. The resultant engine performance was within 2 to 3 percent of the desired value. The principal limitation in obtaining the desired performance was the accuracy with which the controlled diffuser pressure and the average diffuser pressure could be related.

The control system responded satisfactorily to all disturbances imposed, including those which placed the engine well into the diffuser buzz region. Minimum response times approaching the magnitude of the system dead time of 0.035 second were obtained with controller settings approaching the stability limits. Response times as low as 0.1 second were obtained with less than 10 percent overshoot. The instability point was accurately predicted from the experimental frequency response characteristics of the engine and control-system components. With fast control response, brief excursions into the subcritical region were obtained without initiation of diffuser buzz.

The control technique permits the use of any desired schedule of diffuser pressure which calls for operation in the supercritical region and, if applied in conjunction with a limiting device, will also accommodate operation at maximum pressure ratio.

The diffuser static pressure appears to be the most desirable parameter for use in the type of control presented herein, because of the better measurement accuracy possible, a shorter dead time, and a lower noise level.

Lewis Flight Propulsion Laboratory
National Advisory Committee for Aeronautics
Cleveland, Ohio, April 20, 1955

[redacted]

APPENDIX A

SYMBOLS

The following symbols are used in this report:

C_{F-D}	coefficient of net propulsive thrust
K	gain factor
M	Mach number
P	total pressure, lb/sq ft
p	static pressure, lb/sq ft
sfc	specific fuel consumption, lb fuel/hr/lb thrust - drag
S	complex operator
T	total temperature, ^{o}R
V	voltage
V_i	input voltage to fuel servo
W_f	fuel flow, lb/hr
α	angle of attack, deg
Δp_L	$p_b - p_a$, limit-signal pressure
ε	error signal
τ	integrator time constant

Subscripts:

a	1 in. behind cone tip
ac	auxiliary cone
av	average
b	plane of cowl lip
c	control
max	maximum

ref reference

S secondary

T total

x diffuser exit

0 free stream

1 engine inlet

Superscript:

' pressure behind normal shock

APPENDIX B

INSTRUMENTATION

Engine Variables

For the measurement of engine variables during transient operation of the engine, it was necessary to select instruments having fast response in view of the short response times expected. For the measurement of pressures within the engine, pressure transducers of the variable-inductance type having high natural frequencies were selected. Connecting tubing lengths were kept to a minimum, and wherever possible static pressures were measured by transducers screwed directly into the static-pressure tap.

The response characteristics of the pressure transducers were obtained from bench tests of the step-function response of each transducer and its associated tubing and from a limited number of sinusoidal response tests of each type of transducer used with several tubing combinations. The response characteristics for each variable are given in the following table. Where reference is made to the frequency response curves of figures 34 to 36, the data were taken for the specific transducer and tubing used. Where the curve is indicated as approximate, comparison of tubing dimensions and the step-function responses shows sufficient agreement to permit use of the indicated curves. The accuracy of the step-function data given is limited to approximately 0.5 millisecond in measurement of response time and ± 5 percent in overshoot. The step data were recorded with a galvanometer having a natural frequency of 500 cps, damped at 64 percent of critical, which gave a flat response of ± 5 percent at frequencies to 300 cps. Since the galvanometer response is of the same order of magnitude as the possible error in the measurements, no correction has been made in the data for the effect of the galvanometer.

Variable	Transducer type	Frequency response characteristic		Response to step function	
		Figure	Curve	63-Percent point	Percent overshoot
P'_0	I	34(a) and (b)	c	0.0011	60
P'_a	I	34(a) and (b)	c (approx.)	0.0012	60
P'_{ac}	II			0.016	none
P_0	I	34(a) and (b)	A	0.0005	8.6
$\Delta p_L \begin{cases} p_b \\ -p_a \end{cases}$	II	35(a) and (b)	A (approx.)	0.0009 0.014	25.1 none
P_x	I	34(a) and (b)	A	0.0005	8.6
P_x	III	36(a) and (b)	B	0.0041	none

For steady-state performance and transducer calibration these pressures were measured by manometers.

Angle of Attack and Area

For the measurement of angle of attack and exhaust-nozzle area during transient, slide-wire potentiometers connected in a resistance bridge circuit were used. The exit-area indication was obtained by sensing the position of the exit plug, which reduced the area linearly as it was moved into the nozzle. In steady state these variables were measured by counters.

Fuel Variables

Fuel-nozzle pressure drop was measured by resistance strain-gage-type differential pressure transducers connected approximately 8 inches upstream of both the primary and secondary fuel nozzles and referenced to the air pressure in the region of the nozzles. The response of the fuel pressure side of the transducers with tubing was found from bench tests to be flat within ± 5 percent to frequencies of at least 150 cps with no measurable phase shift. For steady-state measurements, fuel pressures were sensed by synchronous-type pressure transmitters, and fuel flow was measured by rotameters.

The input voltage to the fuel servo and the fuel-valve-position signal was measured directly at the fuel-servo control panel and connected to the recorder by means of isolating d-c amplifiers and matching networks to provide the proper sensitivity and damping characteristics for the galvanometers. The frequency response of the amplifiers was flat within ±5 percent to 200 cps.

Transient Recording

All transient measurements were recorded on sensitized paper in a galvanometric oscillograph with galvanometer elements having natural frequencies of 210 to 500 cps, depending on the amount of filtering desired. In addition, certain variables were monitored on a direct inking oscillograph having a flat frequency response of 100 cps.

REFERENCES

1. Himmel, Seymour C.: Some Control Considerations for Ram-Jet Engines. NACA RM E52F10, 1952.

2. Boksenbom, Aaron S., and Novik, David: Control Requirements and Control Parameters for Ram Jet with Variable-Area Exhaust Nozzle. NACA RM E8H24, 1948.

3. Vasu, G., Wilcox, F. A., and Himmel, S. C.: Preliminary Report of Experimental Investigation of Ram-Jet Controls and Engine Dynamics. NACA RM E54H10, 1954.

4. Hearth, Donald P., and Perchonok, Eugene: Performance of a 16-Inch Ram-Jet Engine with a Can-Type Combustor at Mach Numbers of 1.50 to 2.16. NACA RM E54G13, 1954.

5. Otto, Edward W., Gold, Harold, and Hiller, Kirby W.: Design and Performance of Throttle-Type Fuel Controls for Engine Dynamic Studies. NACA TN 3445, 1955.

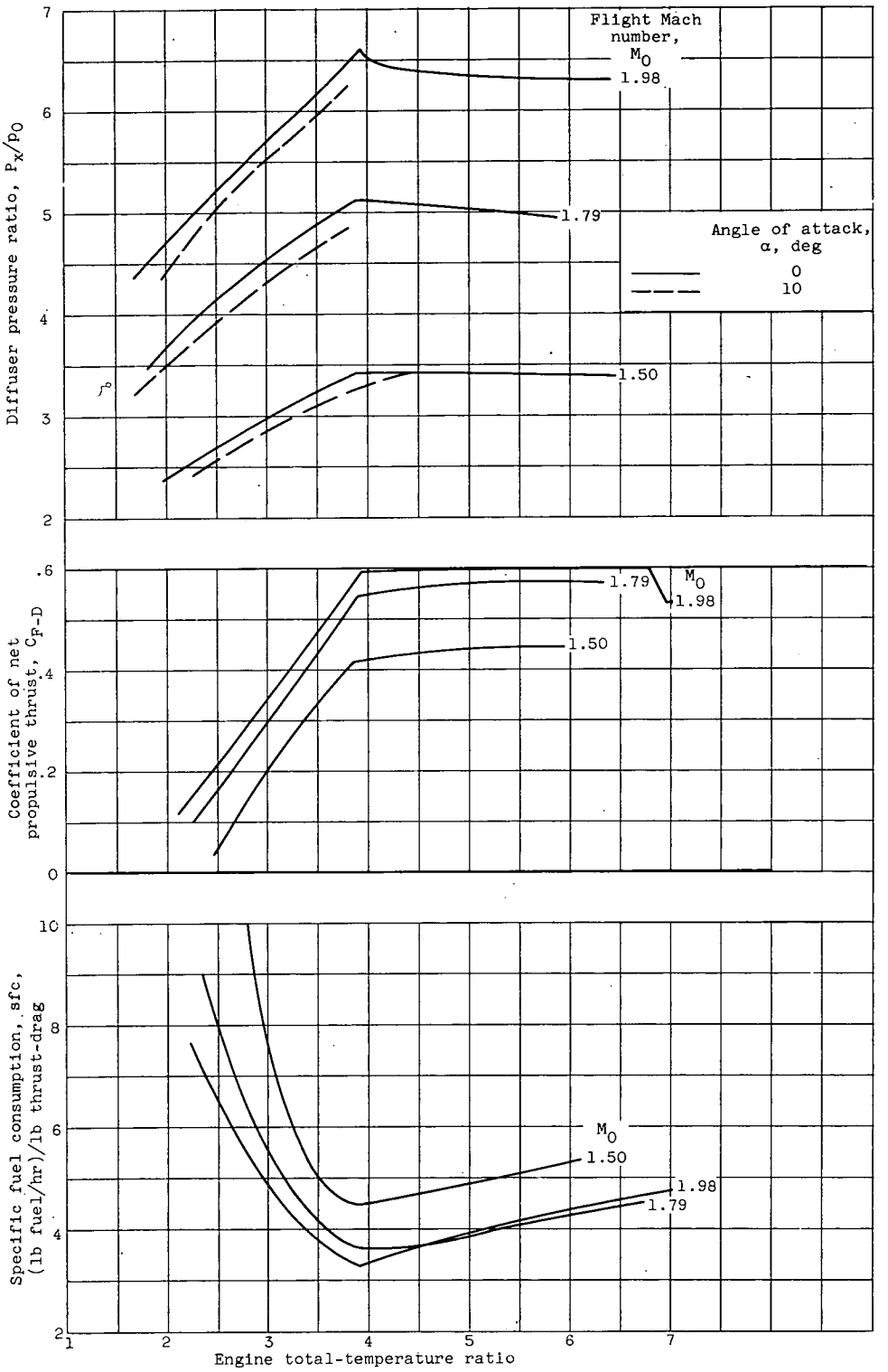

Figure 1. - Engine performance map for 16-inch ram-jet engine. Exhaust-nozzle area, 0.960 square foot.

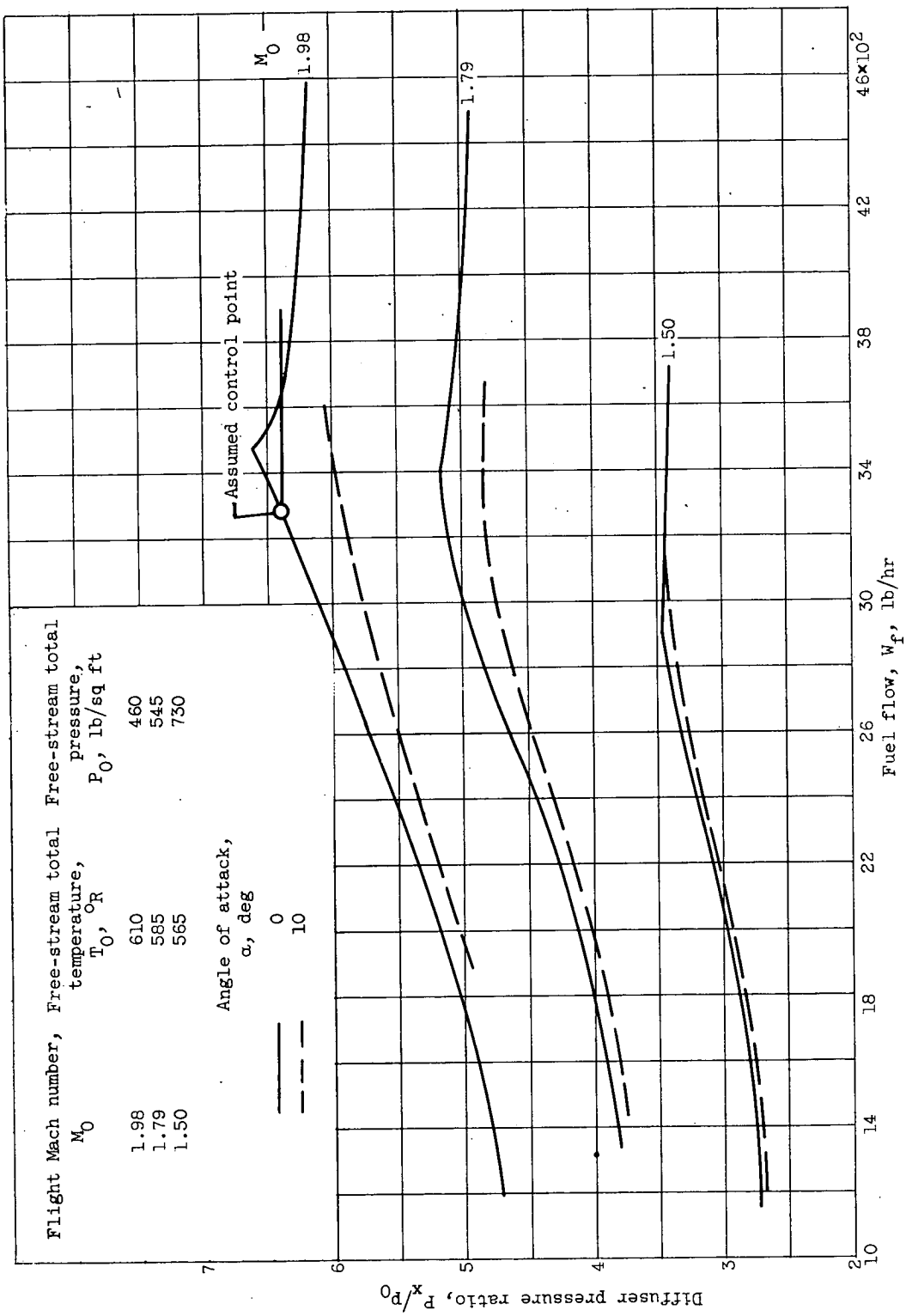

Figure 2. - Variation of diffuser pressure ratio with fuel flow in 16-inch ram-jet engine. Exhaust-nozzle area, 0.960 square foot.

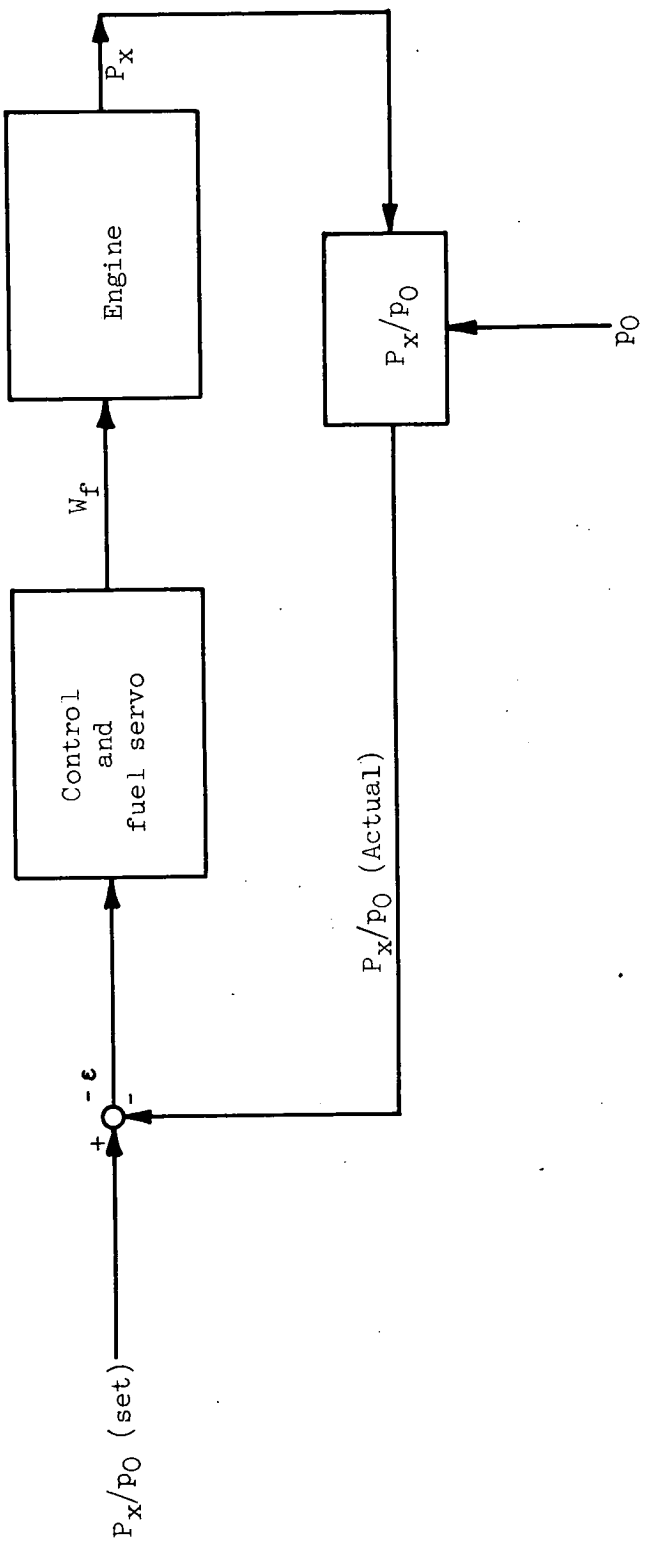

Figure 3. - Simplified block diagram of diffuser-pressure-ratio control.

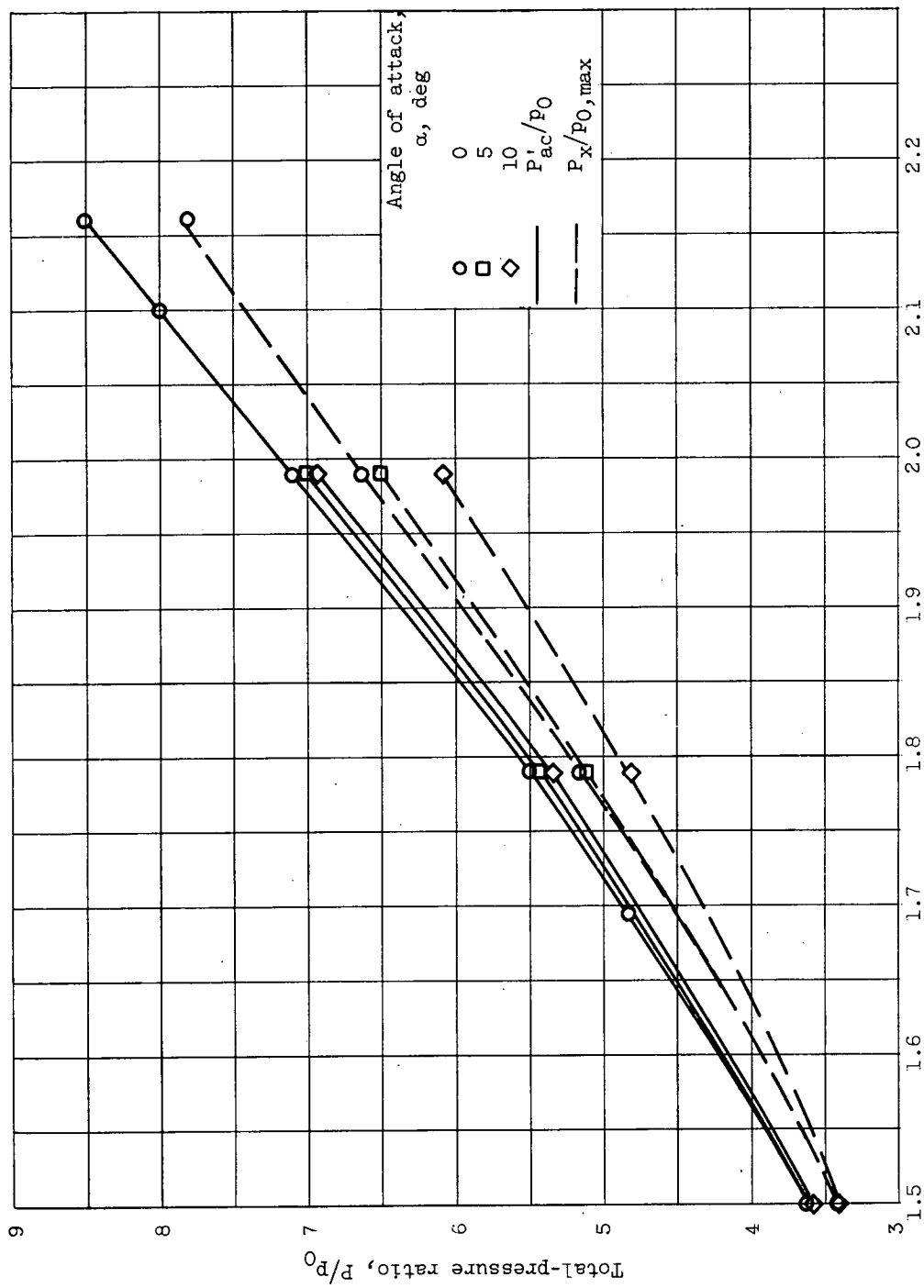

Figure 4. - Variation of reference pressure ratio P'_{ac}/p_0 and maximum average diffuser pressure ratio $P_x/p_{0,max}$ with flight Mach number and angle of attack.

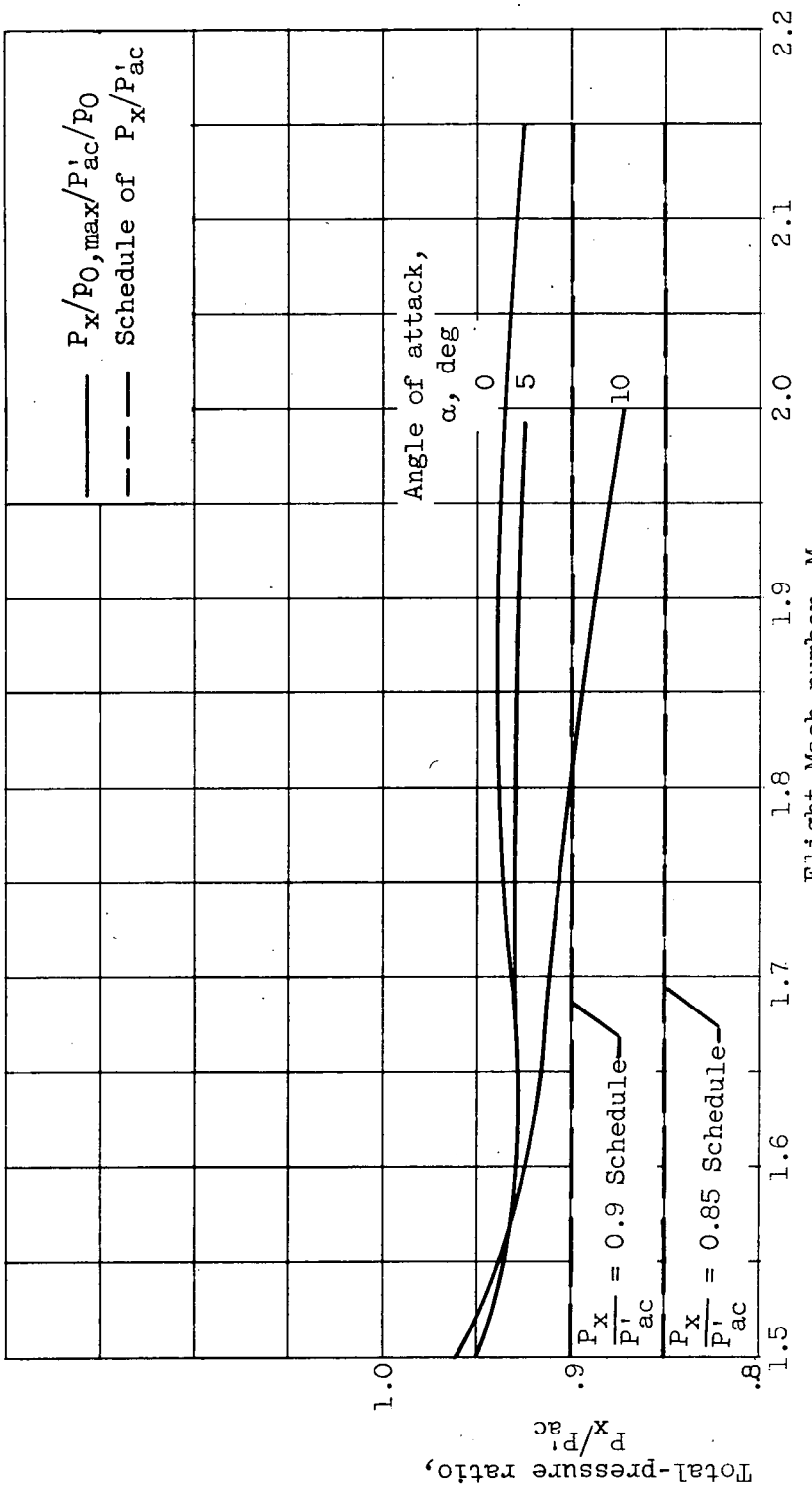

Figure 5. - Variation of ratio of diffuser-exit maximum pressure to auxiliary-cone pressure with flight Mach number and angle of attack.

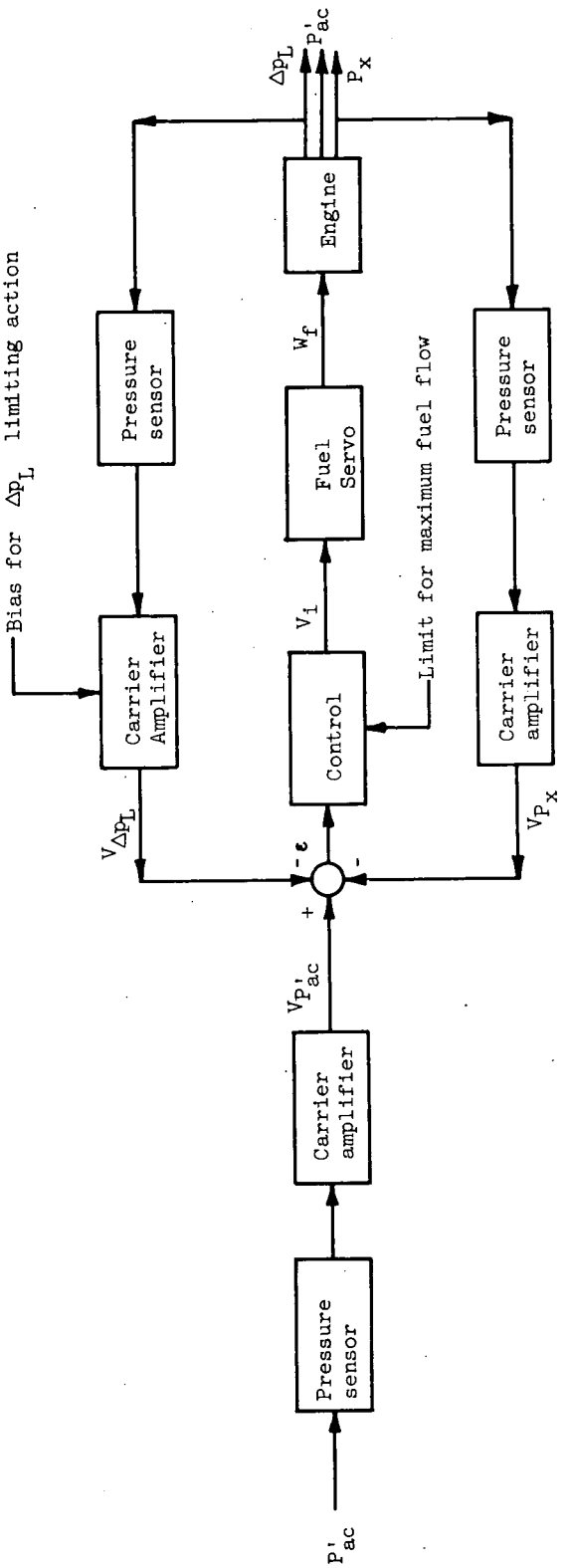

(a) Block diagram.

Figure 6. - Diagrams of diffuser pressure control with shock-position and maximum-fuel-flow limits.

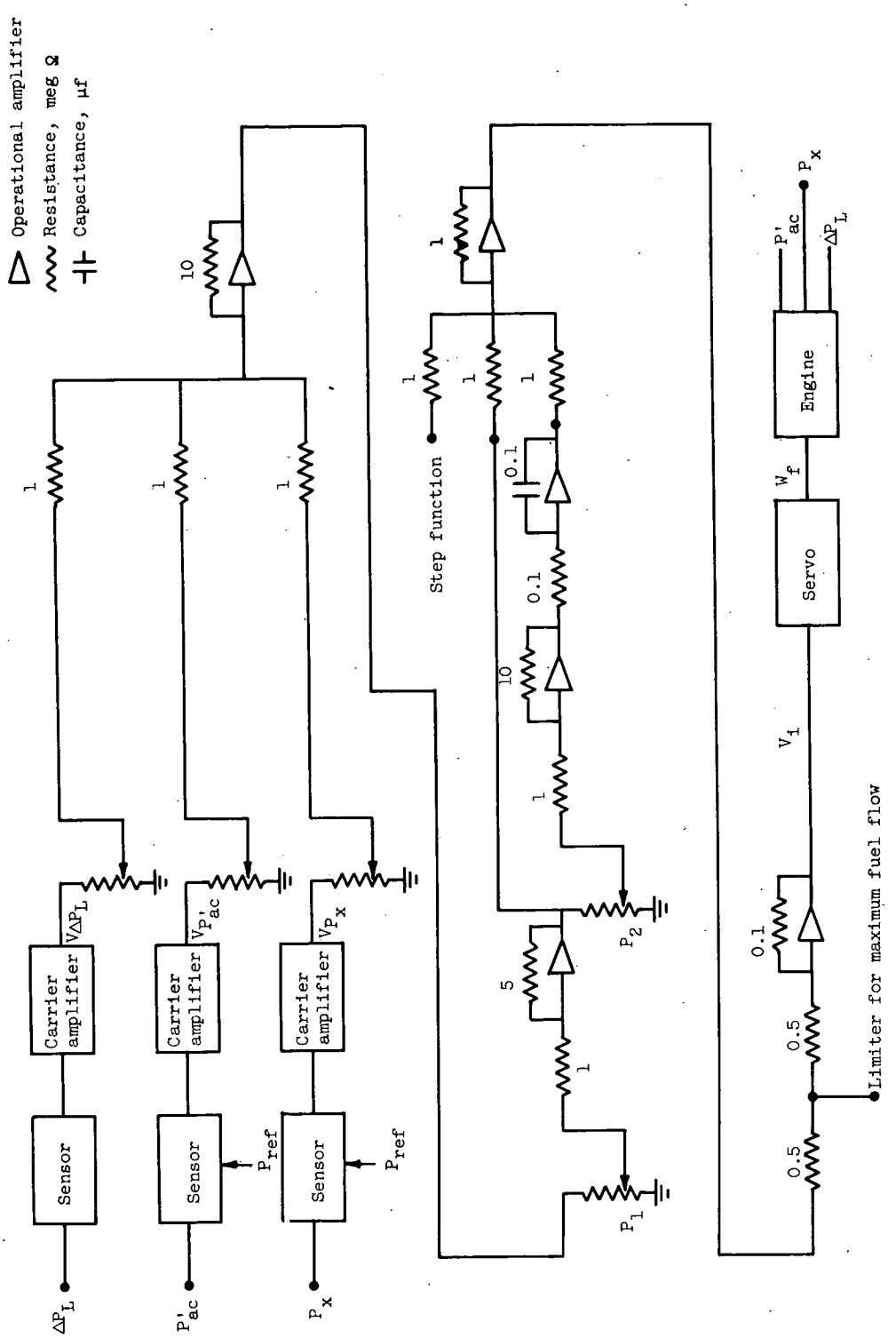

(b) Connection diagram.

Figure 6. - Concluded. Diagrams of diffuser pressure control with shock-position and maximum-fuel-flow limits.

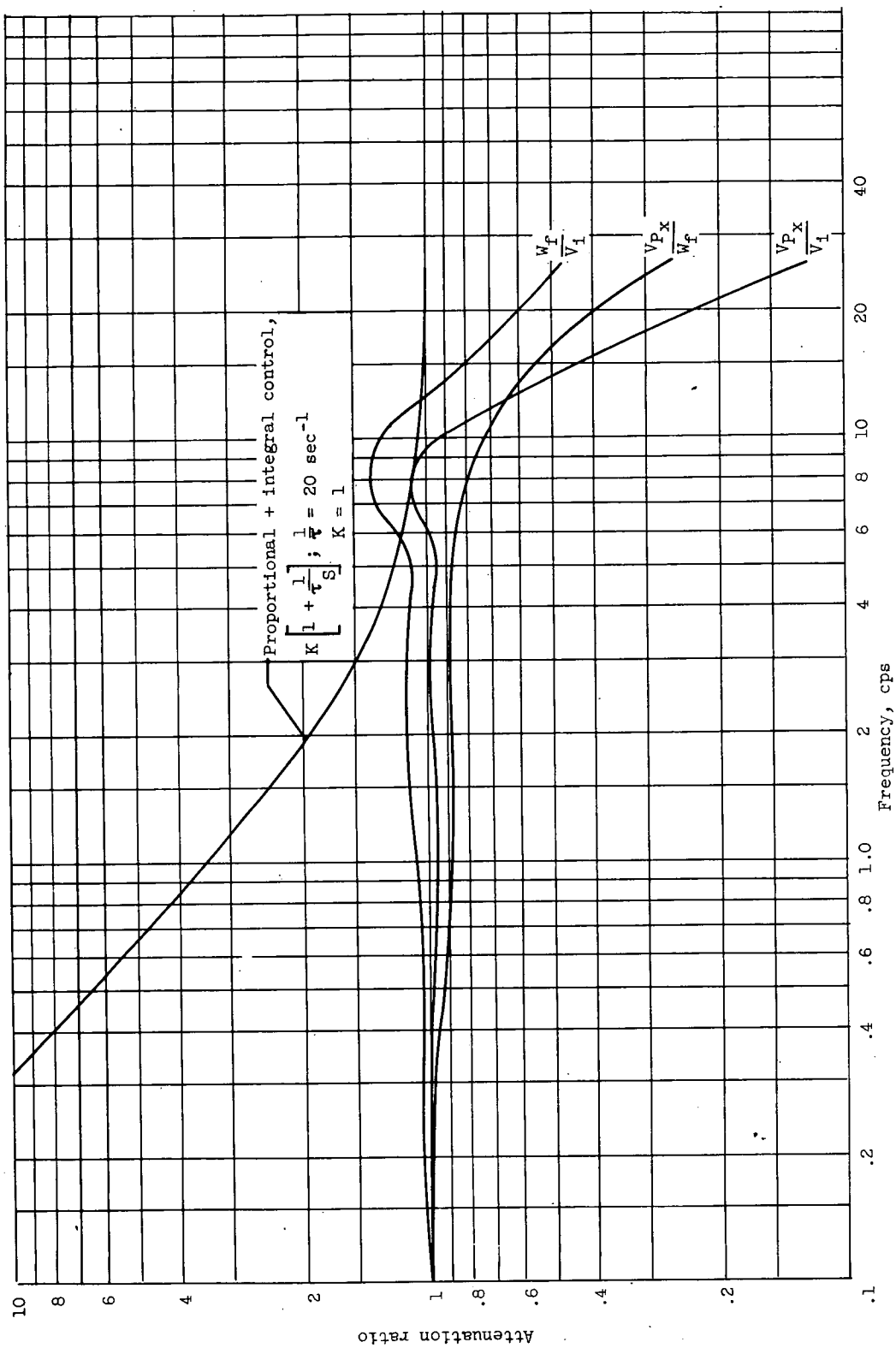

(a) Attenuation frequency.

Figure 7. - Frequency characteristics of control-loop components. Free-stream Mach number, 1.5; zero angle of attack; operating point, 0.9 schedule; integrator time constant, τ, 1/20 second; gain factor, K = 1.

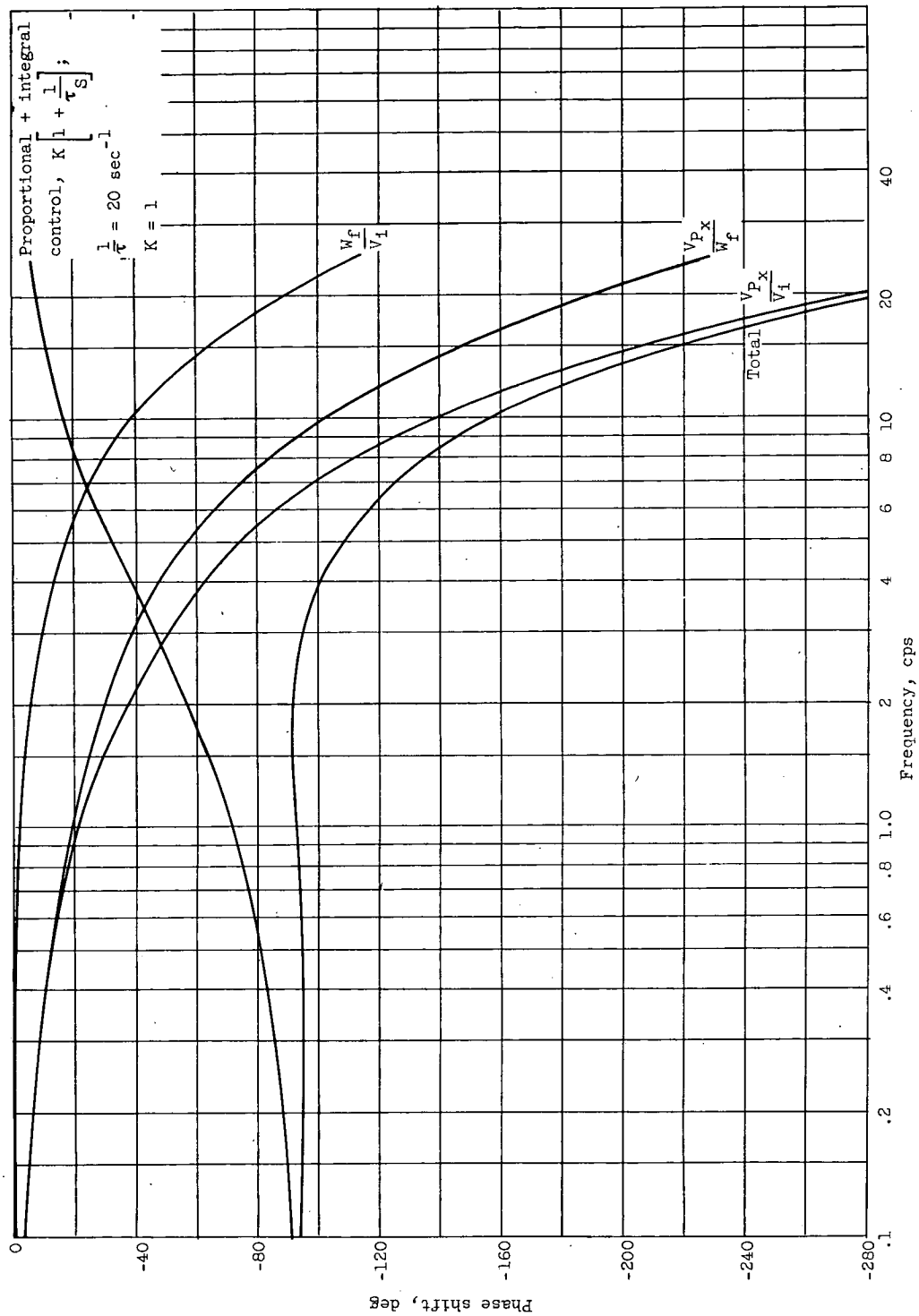

(b) Phase-shift frequency.

Figure 7. - Concluded. Frequency characteristics of control-loop components. Free-stream Mach number, 1.5; zero angle of attack; operating point, 0.9 schedule; integrator time constant, τ, 1/20 second; gain factor K, 1.

[redacted]

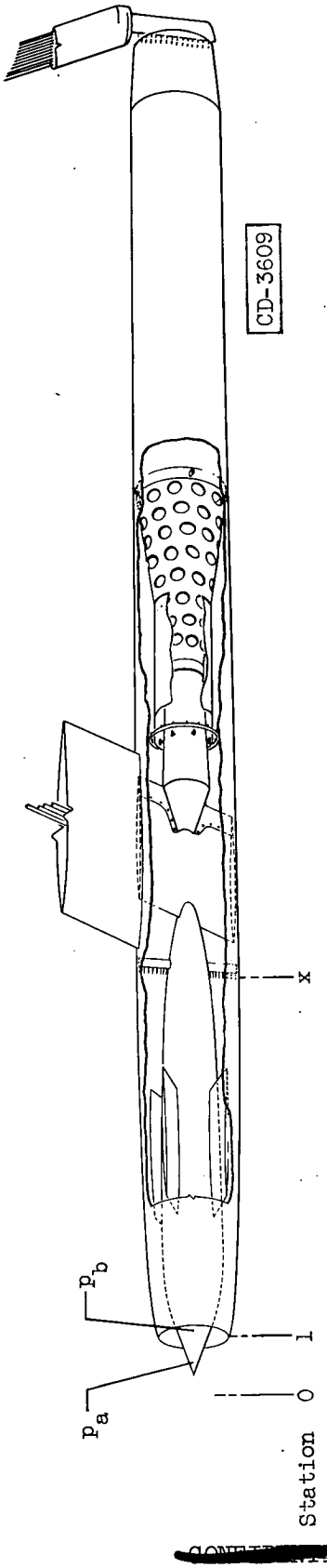

Figure 8. - Engine internal details.

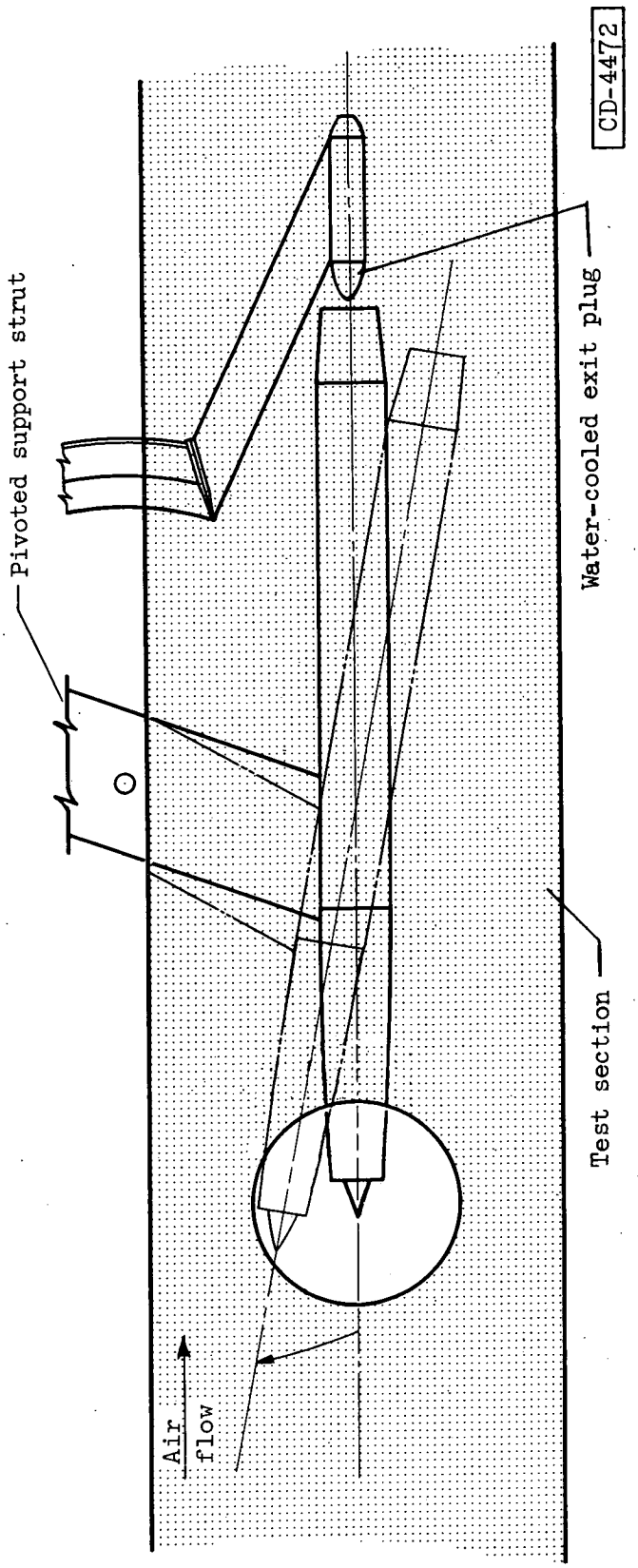

Figure 9. - Installation of 16-inch ram-jet engine in 8- by 6-foot supersonic wind tunnel.

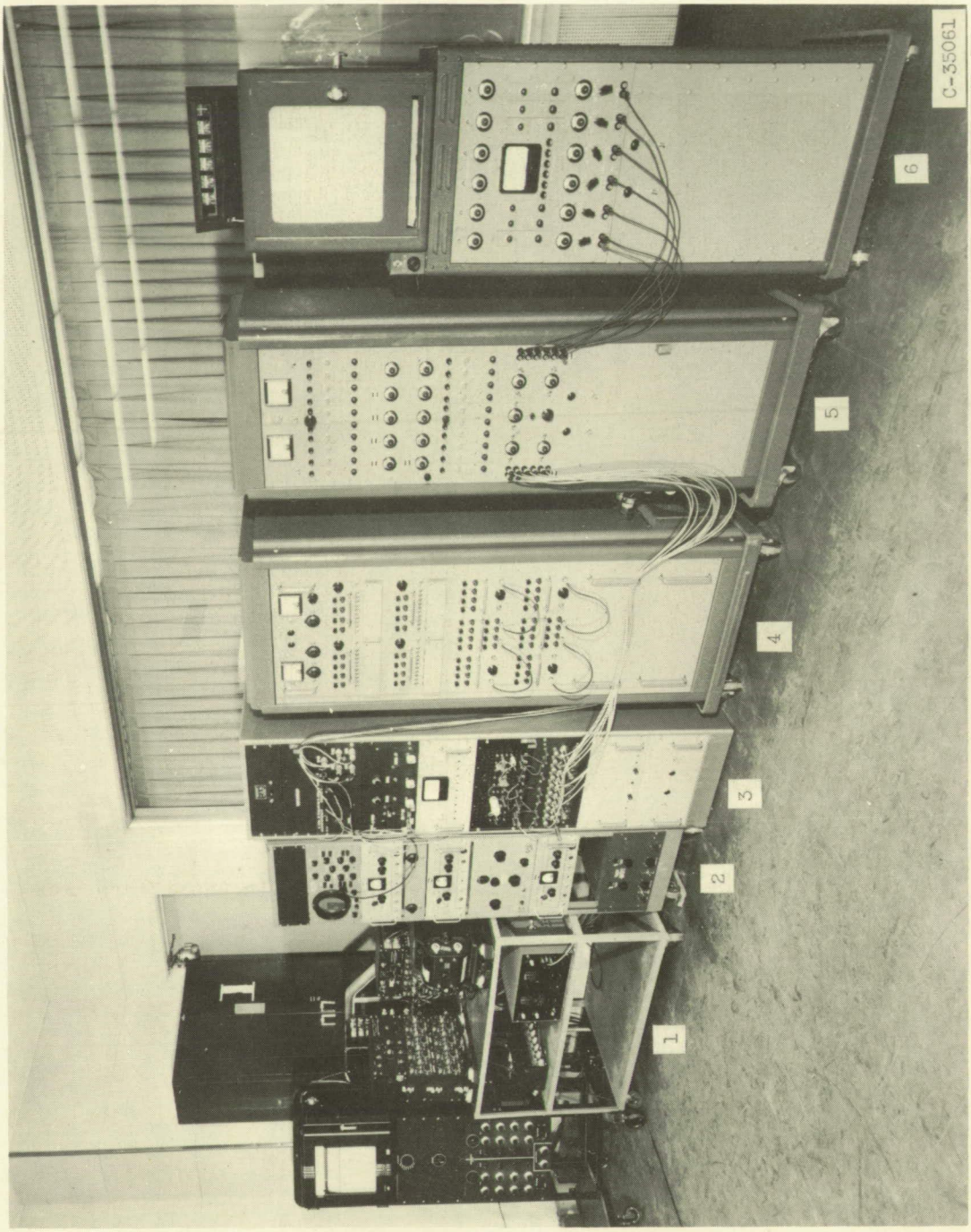

Figure 10. - Control computer and equipment.

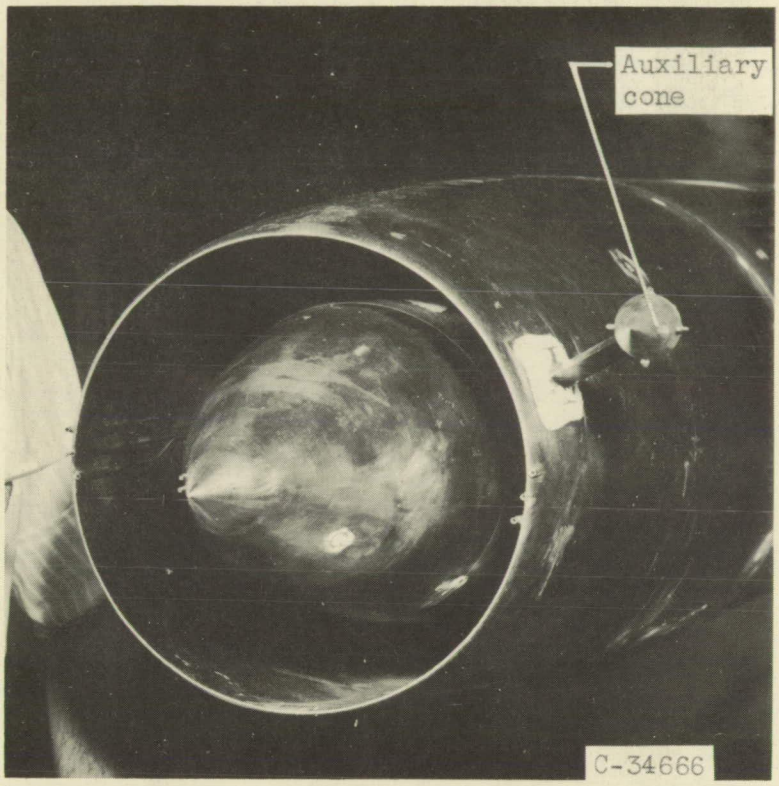

Figure 11. - Front view of 16-inch ram-jet engine showing auxiliary cone.

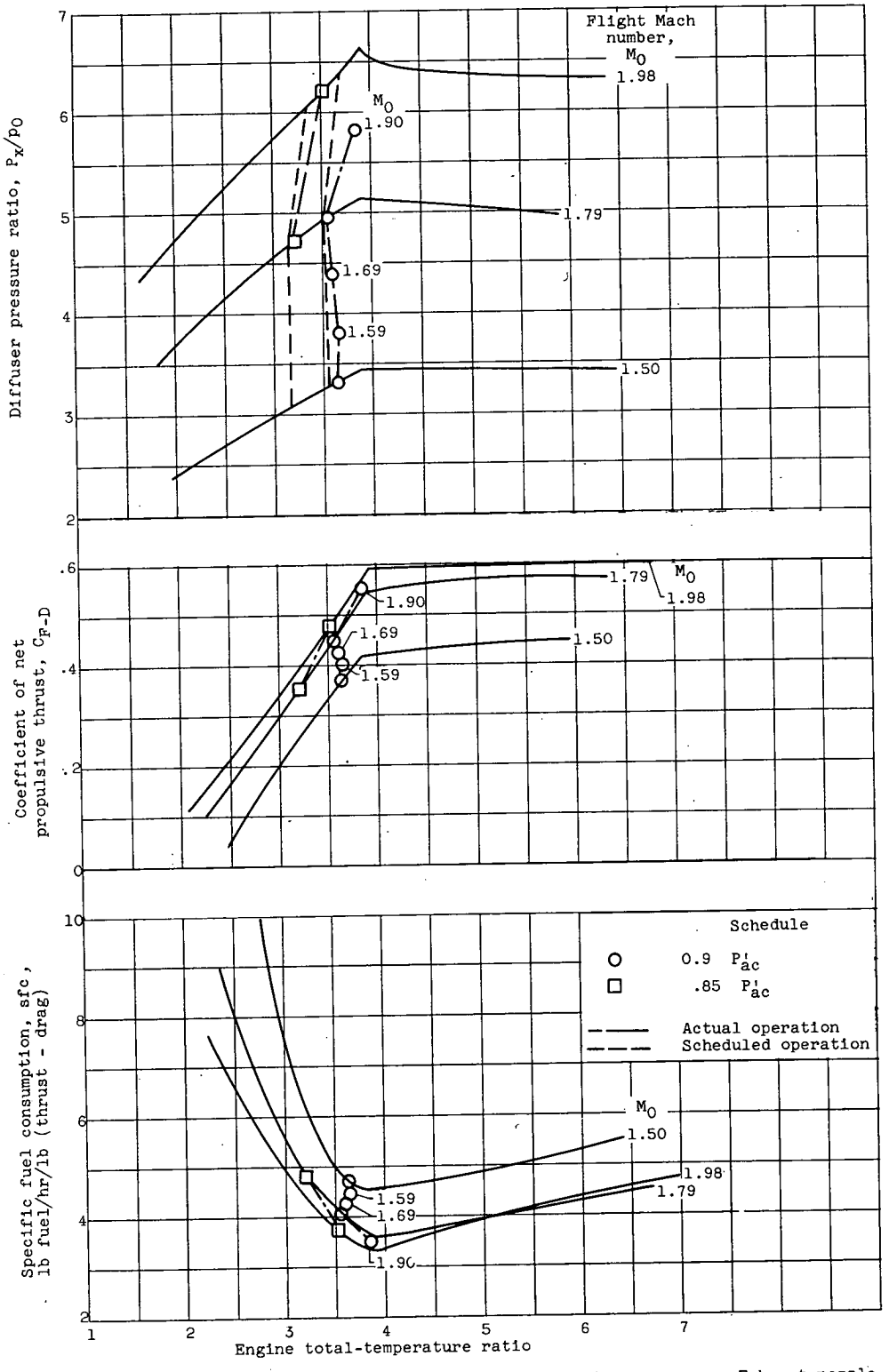

Figure 12. - Control operating points on engine performance map. Exhaust-nozzle area, 0.960 square foot.

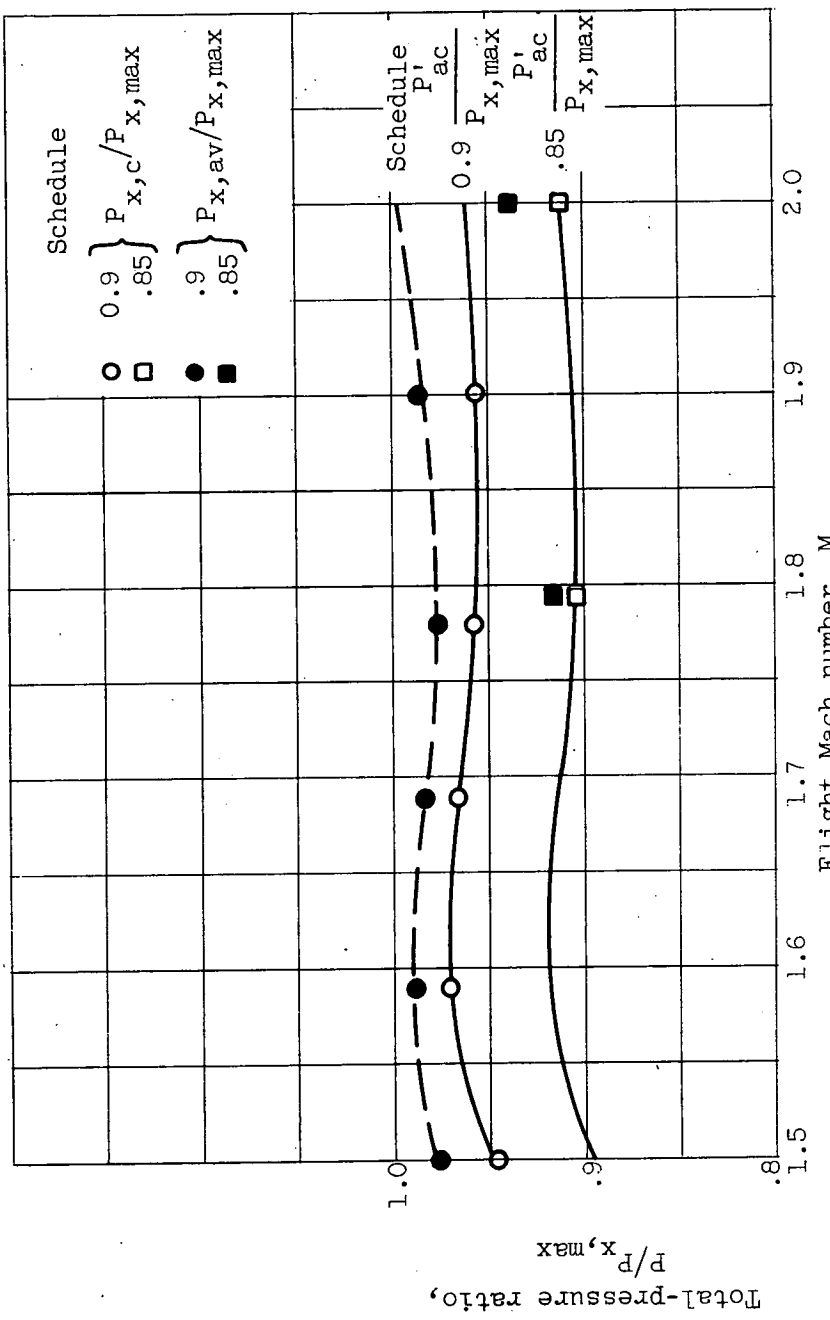

Figure 13. - Deviation of control from scheduled performance.

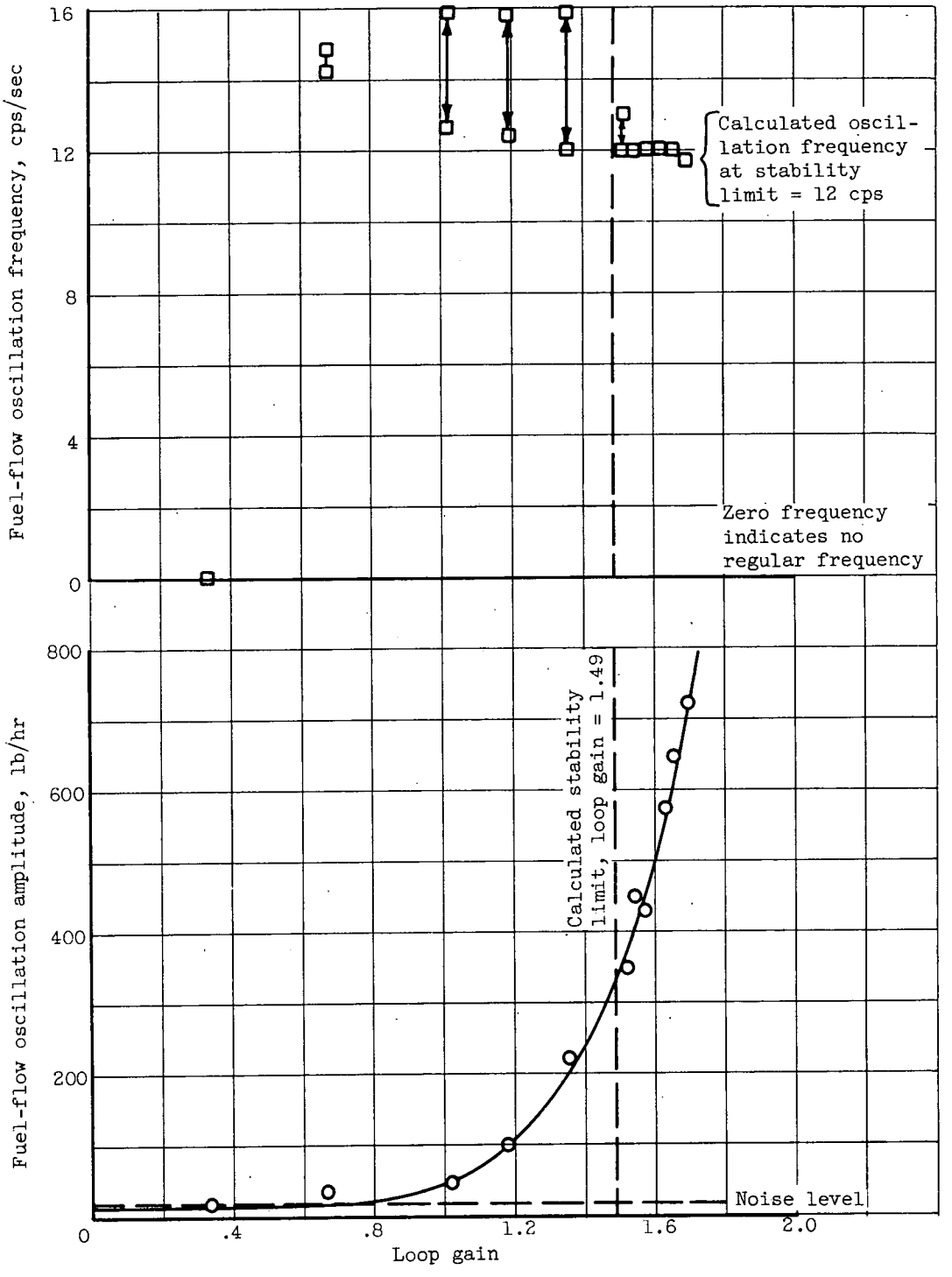

Figure 14. - Oscillation-amplitude and frequency characteristics of control system for fixed integrator time constant $1/\tau = 20$ sec^{-1} and variable proportional loop gain. Flight Mach number, 1.5; zero angle of attack; 0.9 P'_{ac} schedule.

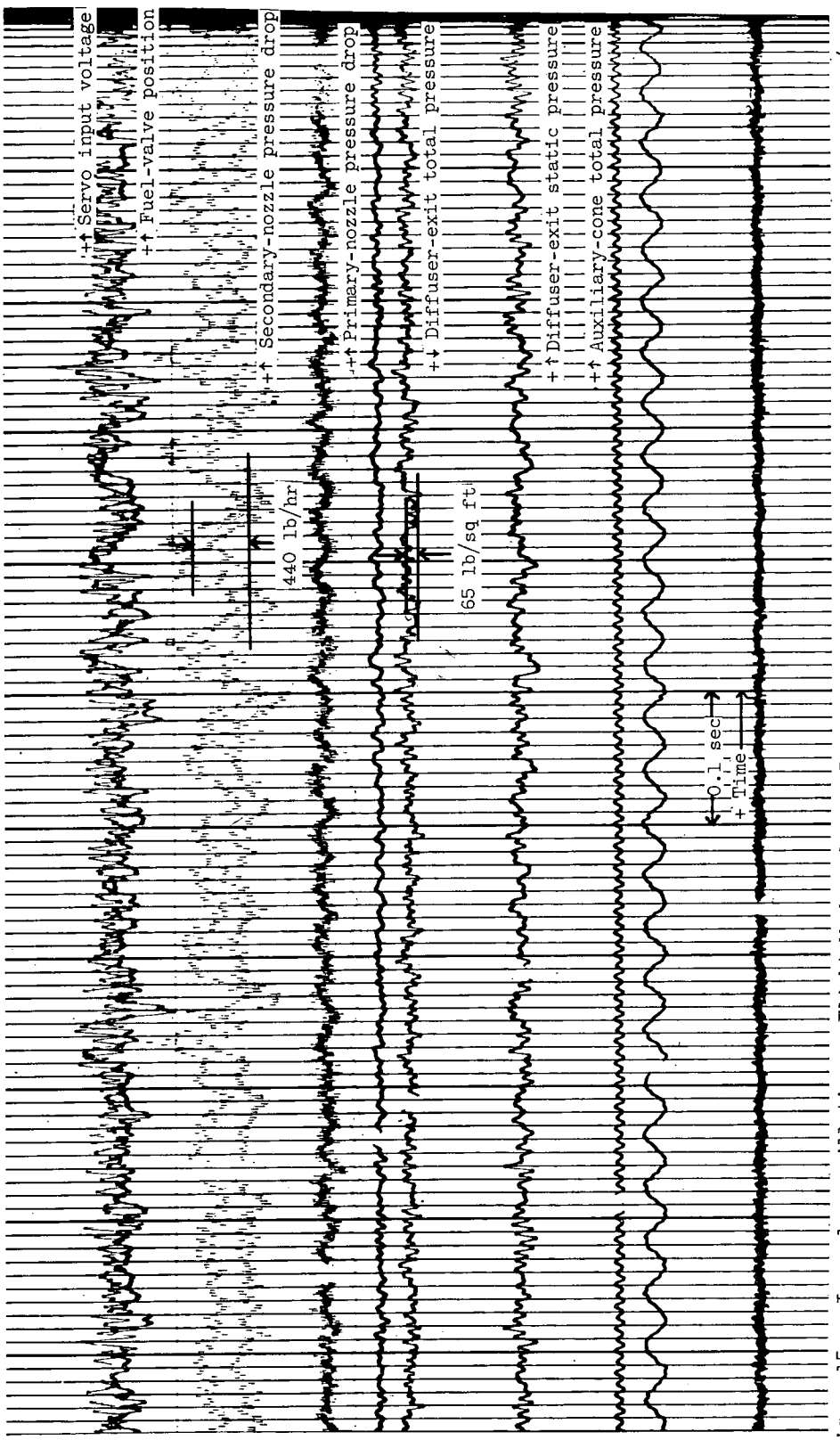

Figure 15. - Irregular oscillations. Flight Mach number, 1.5; zero angle of attack; 0.9 P'_{ac} schedule; loop gain, 1.36; $1/\tau$, 20 sec^{-1}.

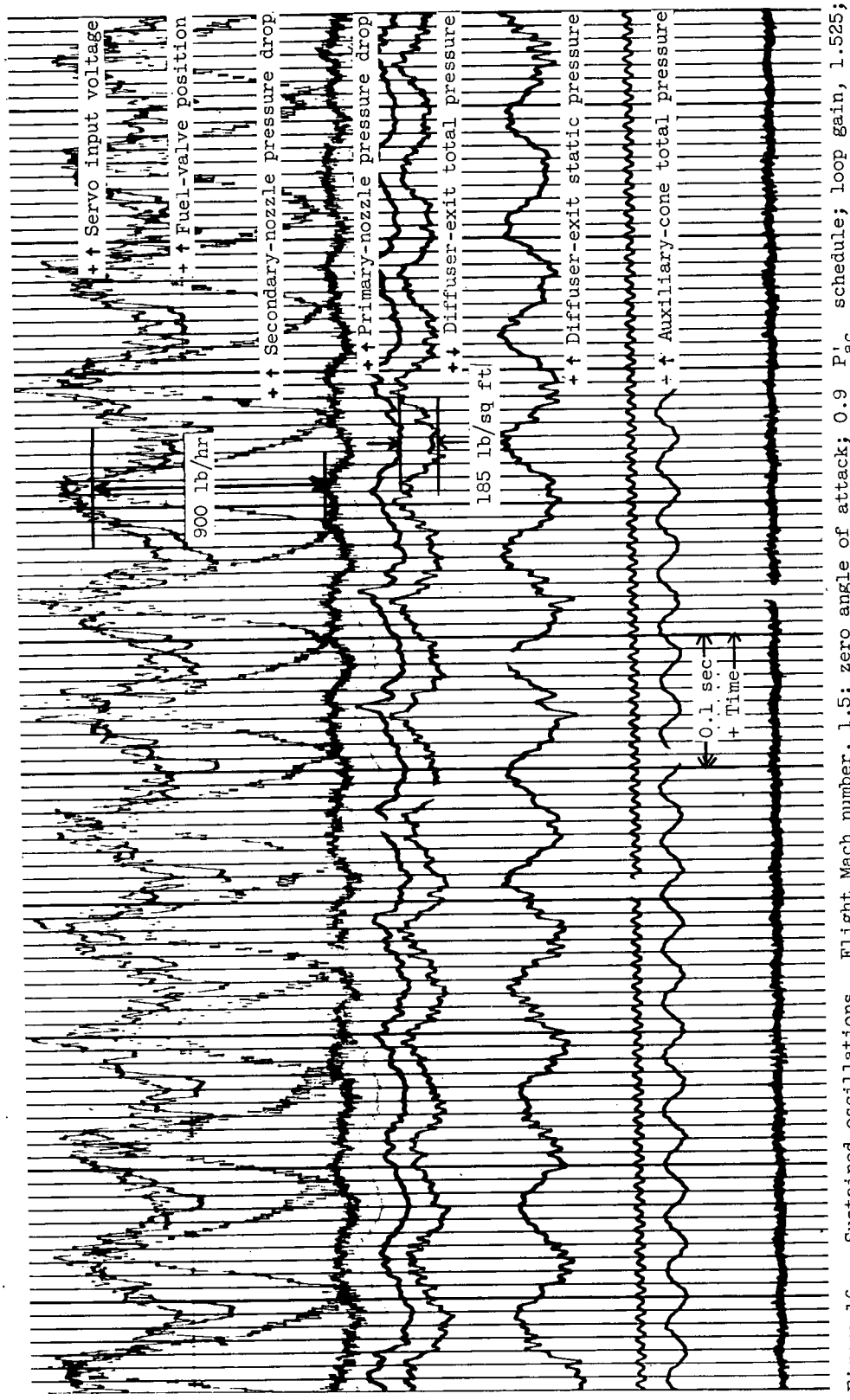

Figure 16. - Sustained oscillations. Flight Mach number, 1.5; zero angle of attack; 0.9 P'_{ac} schedule; loop gain, 1.525; $1/\tau$, 20 sec^{-1}.

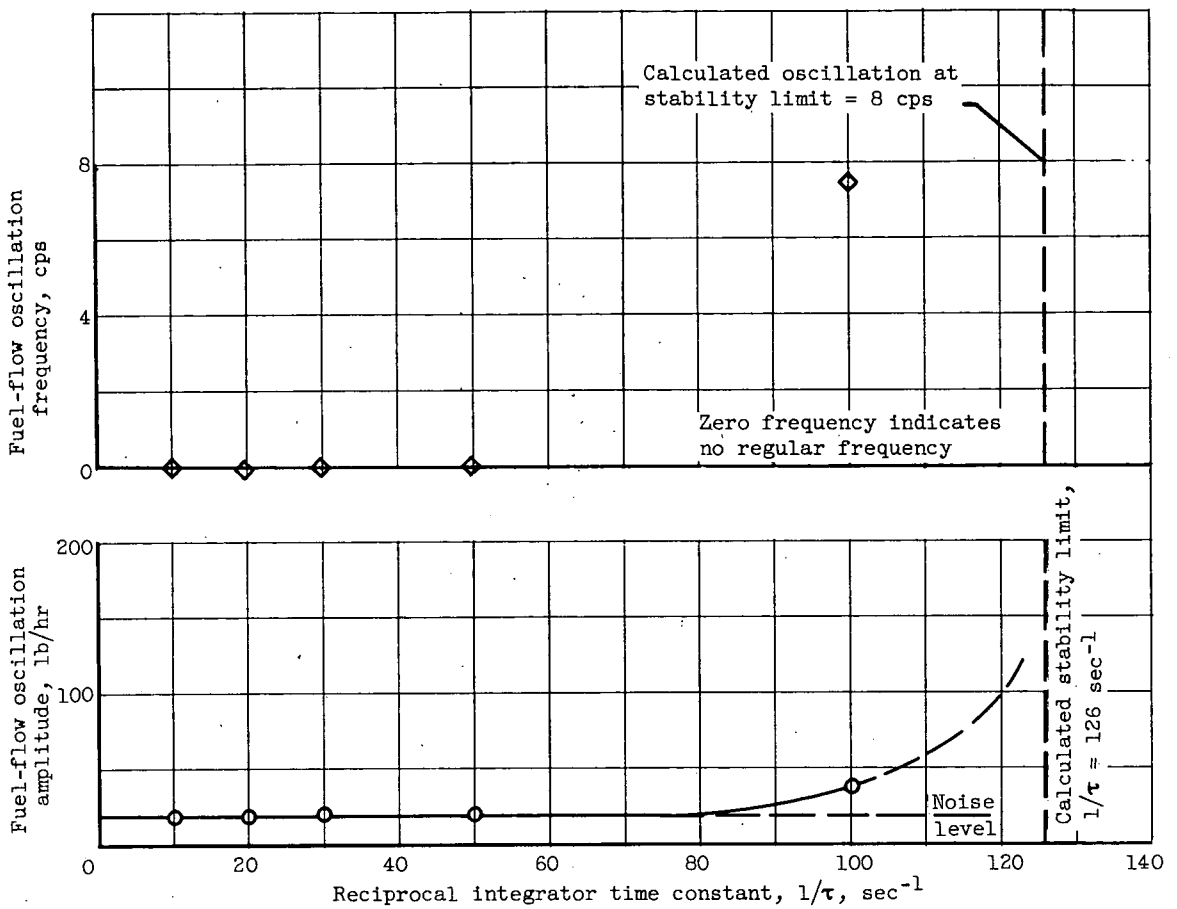

Figure 17. - Oscillation-amplitude and frequency characteristics of control system for fixed proportional loop gain of 0.339 and variable integrator time constant. Flight Mach number, 1.5; zero angle of attack; 0.9 P'_{ac} schedule.

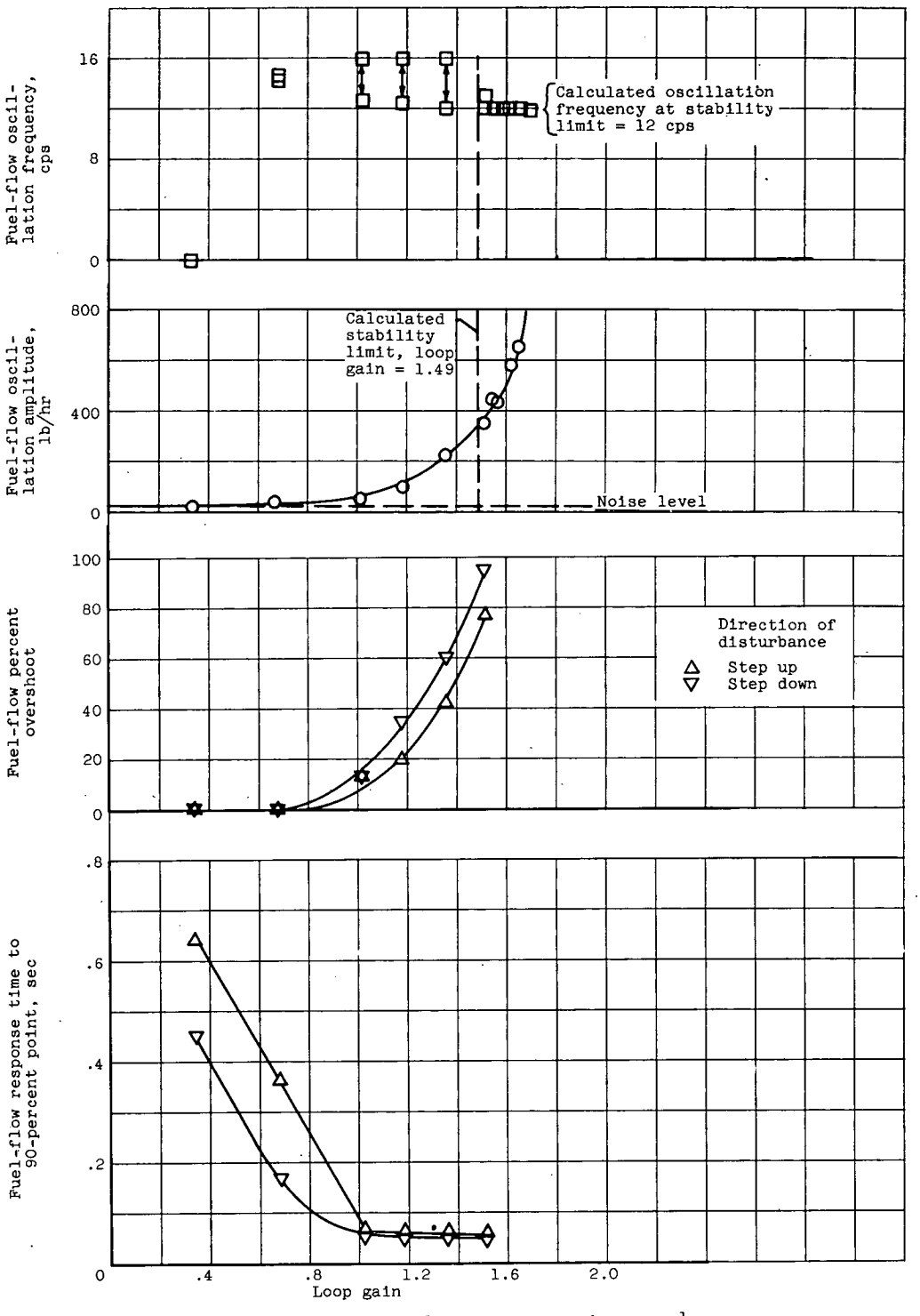

(a) Variable loop gain; $1/\tau'$, 20 sec^{-1}.

Figure 18. - System response characteristic to step disturbance in input voltage to fuel servo of ±2 volts (i.e., fuel-flow step, ±556 lb/hr). Flight Mach number, 1.5; zero angle of attack; 0.9 P'_{ac} schedule.

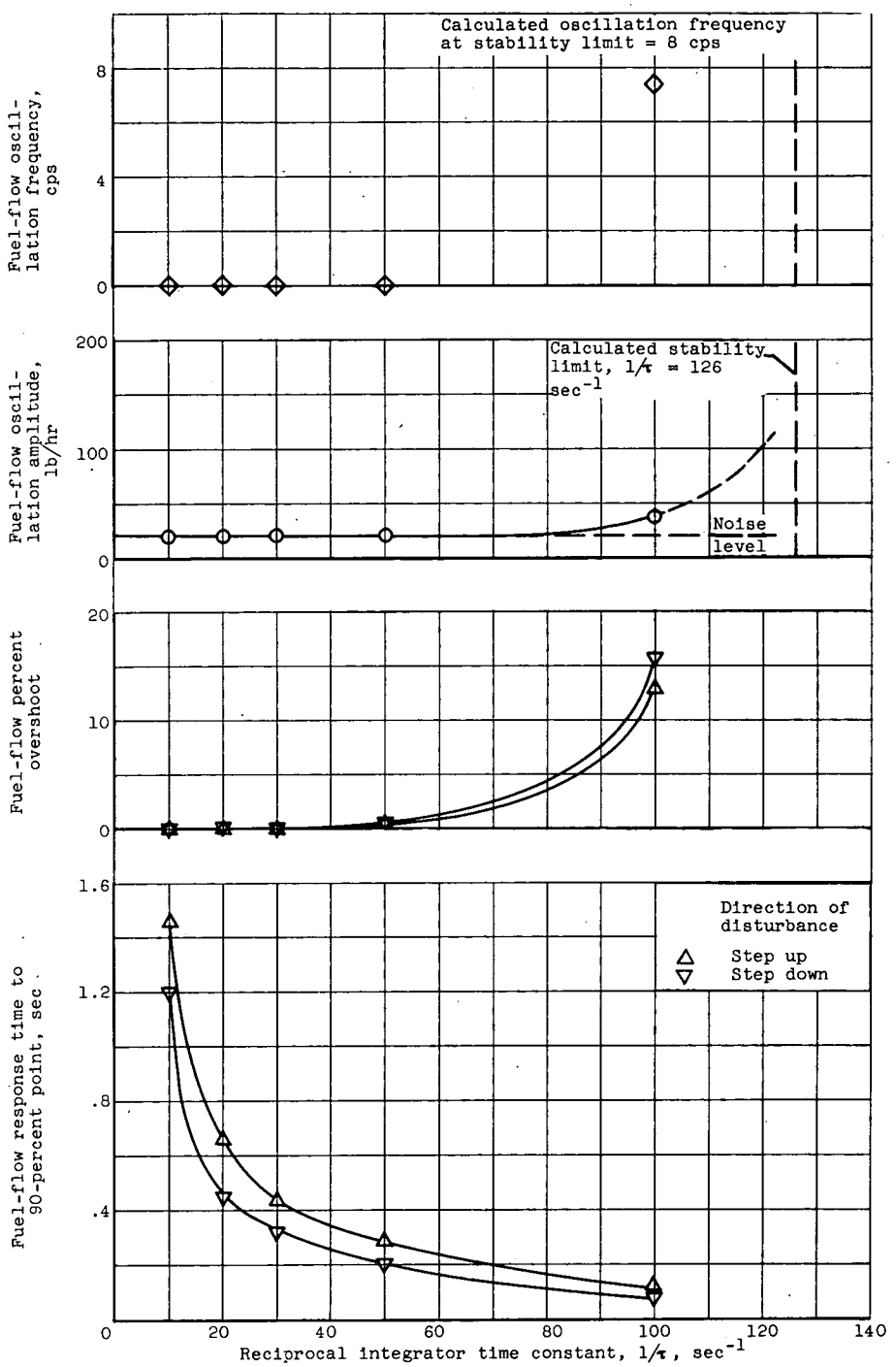

(b) Variable τ; loop gain, 0.339.

Figure 18. - Concluded. System response characteristic to step disturbance in input voltage to fuel servo of ±2 volts (i.e., fuel-flow step, ±556 lb/hr). Flight Mach number, 1.5; zero angle of attack; 0.9 P'_{ac} schedule.

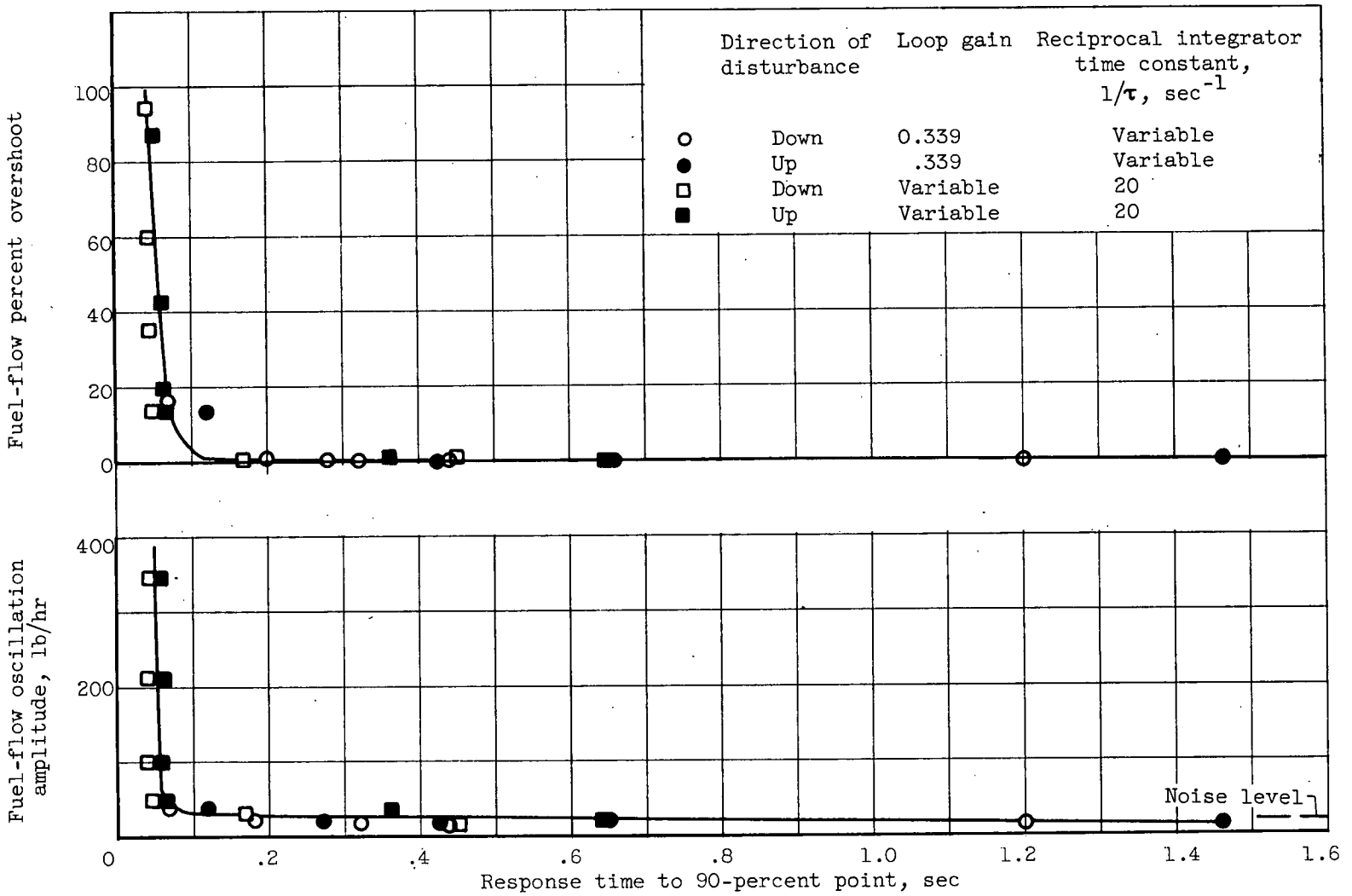

Figure 19. - Oscillation amplitude and percent overshoot as function of response time. Flight Mach number, 1.5; zero angle of attack; 0.9 P'_{ac} schedule.

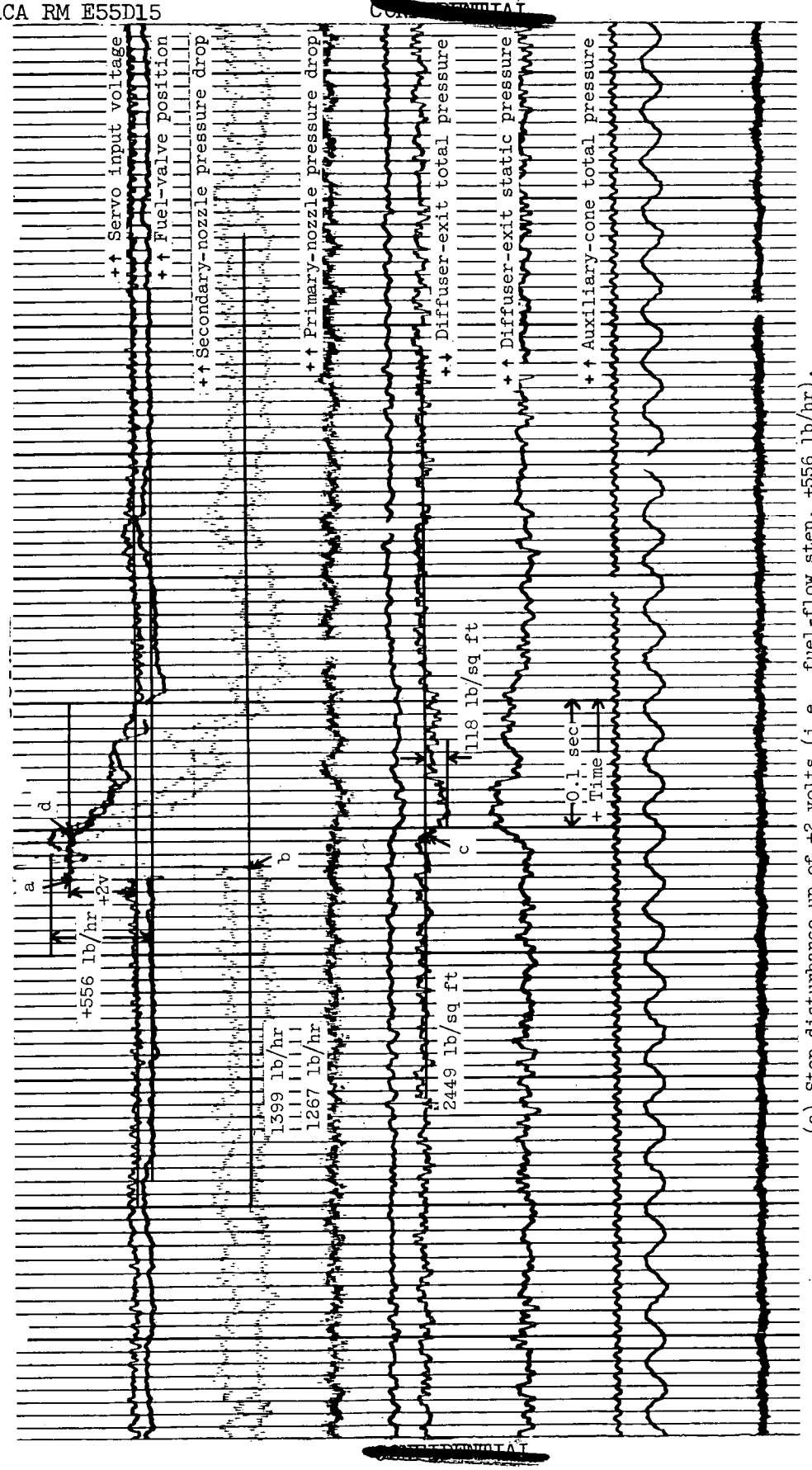

(a) Step disturbance up of +2 volts (i.e., fuel-flow step, +556 lb/hr).

Figure 20. - Response of control to step in servo input voltage. Flight Mach number, 1.5; zero angle of attack; 0.9 P'_{ac} schedule; free-stream static pressure, 758 pounds per square foot; loop gain, 0.339; $1/\tau$, 100 sec^{-1}.

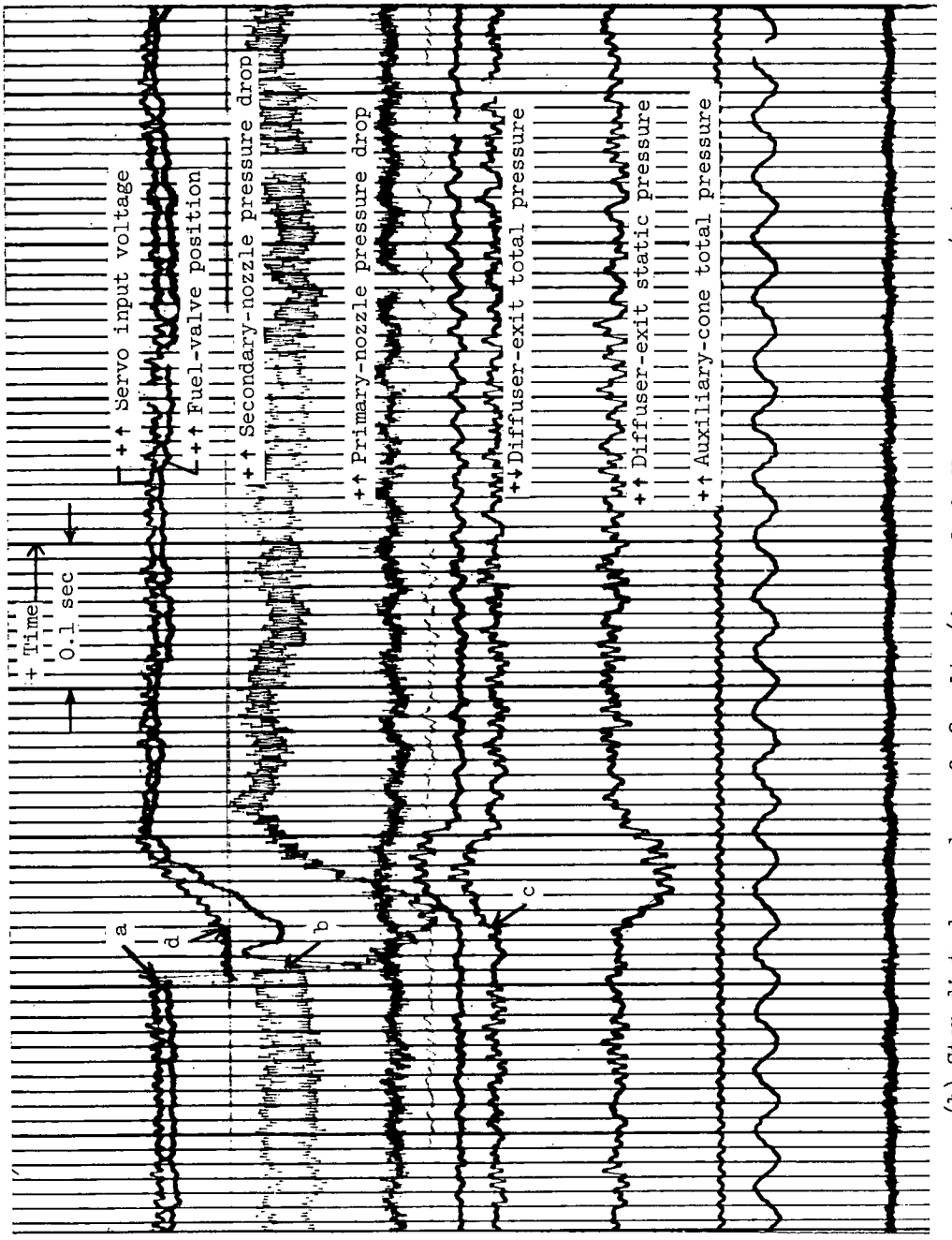

(b) Step disturbance down of -2 volts (i.e., fuel-flow step, -556 lb/hr).

Figure 20. - Concluded. Response of control to step in servo input voltage. Flight Mach number, 1.5; zero angle of attack; 0.9 P'_{ac} schedule; free-stream static pressure, 758 pounds per square foot; loop gain, 0.339; $1/\tau$, 100 sec^{-1}.

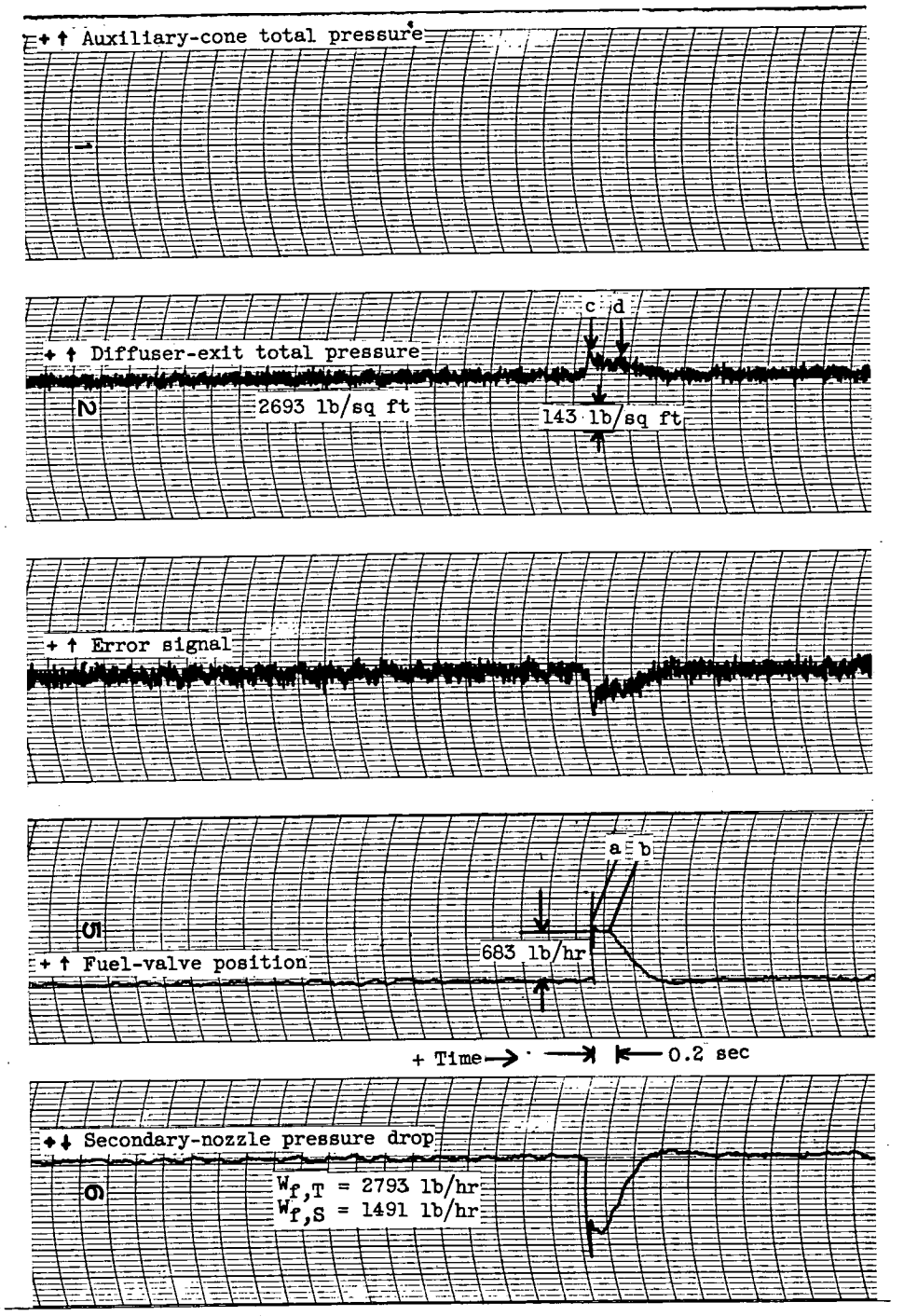

Figure 21. - Operation of fixed fuel-flow limit in controlled system. Flight Mach number, 1.7; zero angle of attack; 0.85 P'_{ac} schedule; free-stream static pressure, 616 pounds per square foot; loop gain, 0.325; $1/\tau$, 50 sec^{-1}.

[redacted]

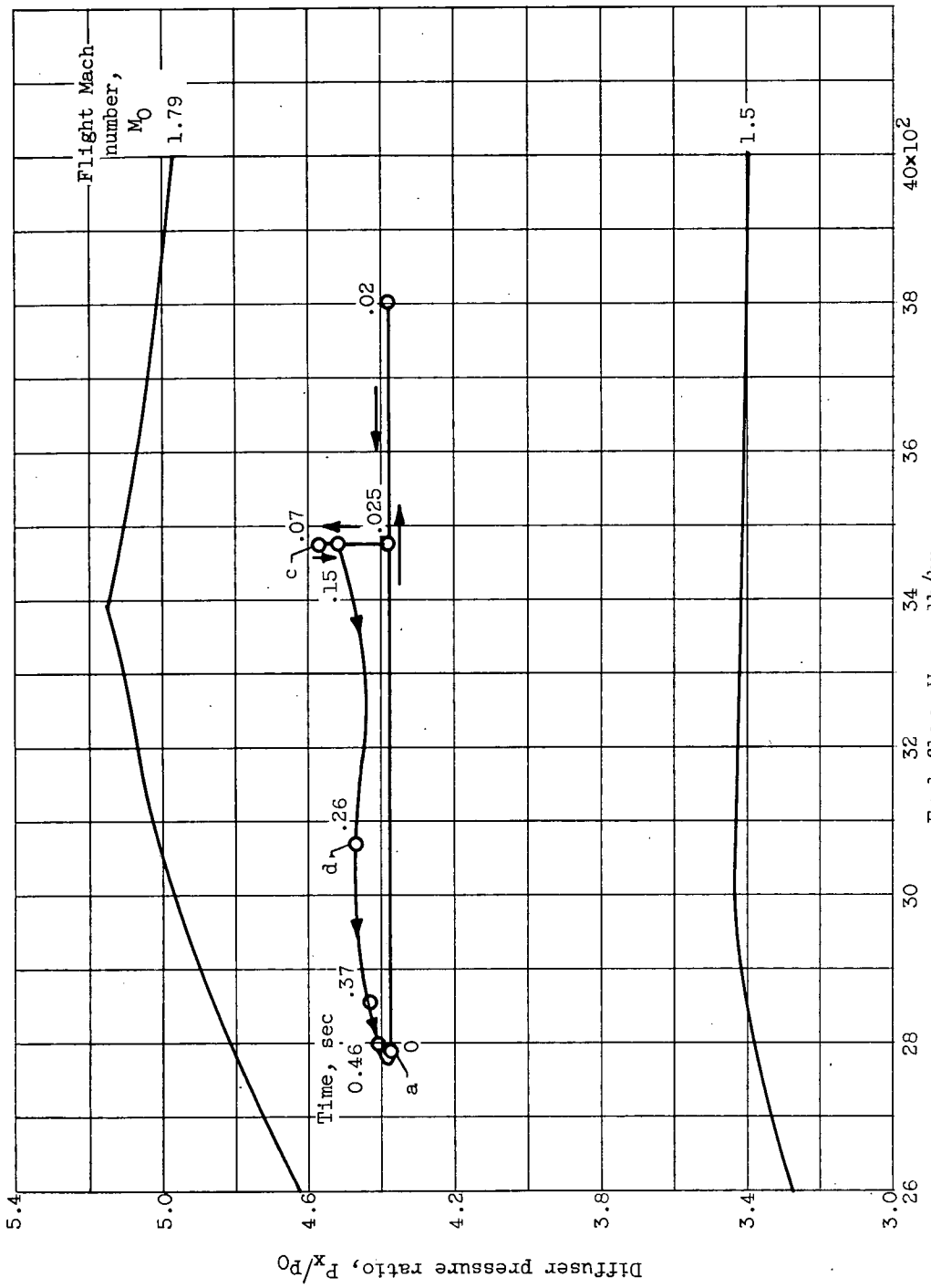

Figure 22. - Superposition of transient of figure 21 on diffuser performance map. Flight Mach number, 1.7; zero angle of attack; loop gain, 0.325; $1/\tau$, 50 sec^{-1}; step disturbance, +4 volts or +1112 pounds per hour; fuel-flow limit set, 3475 pounds per hour.

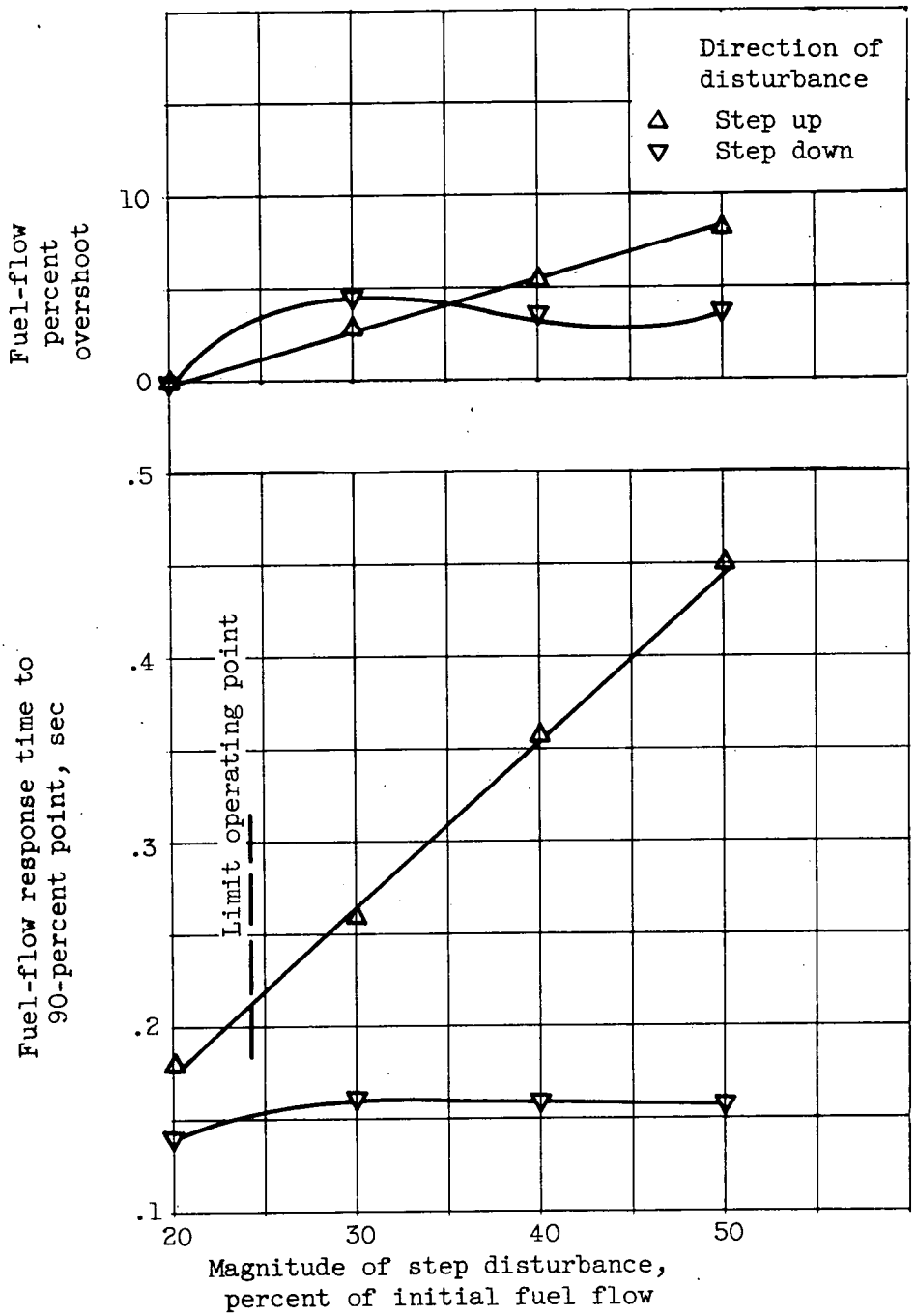

Figure 23. - Control-system response as function of magnitude of disturbance with fixed maximum fuel-flow limit. Flight Mach number, 1.7; zero angle of attack; 0.9 P'_{ac} schedule; loop gain, 0.337; $1/\tau$, 50 sec^{-1}; initial fuel flow, 2793 pounds per hour.

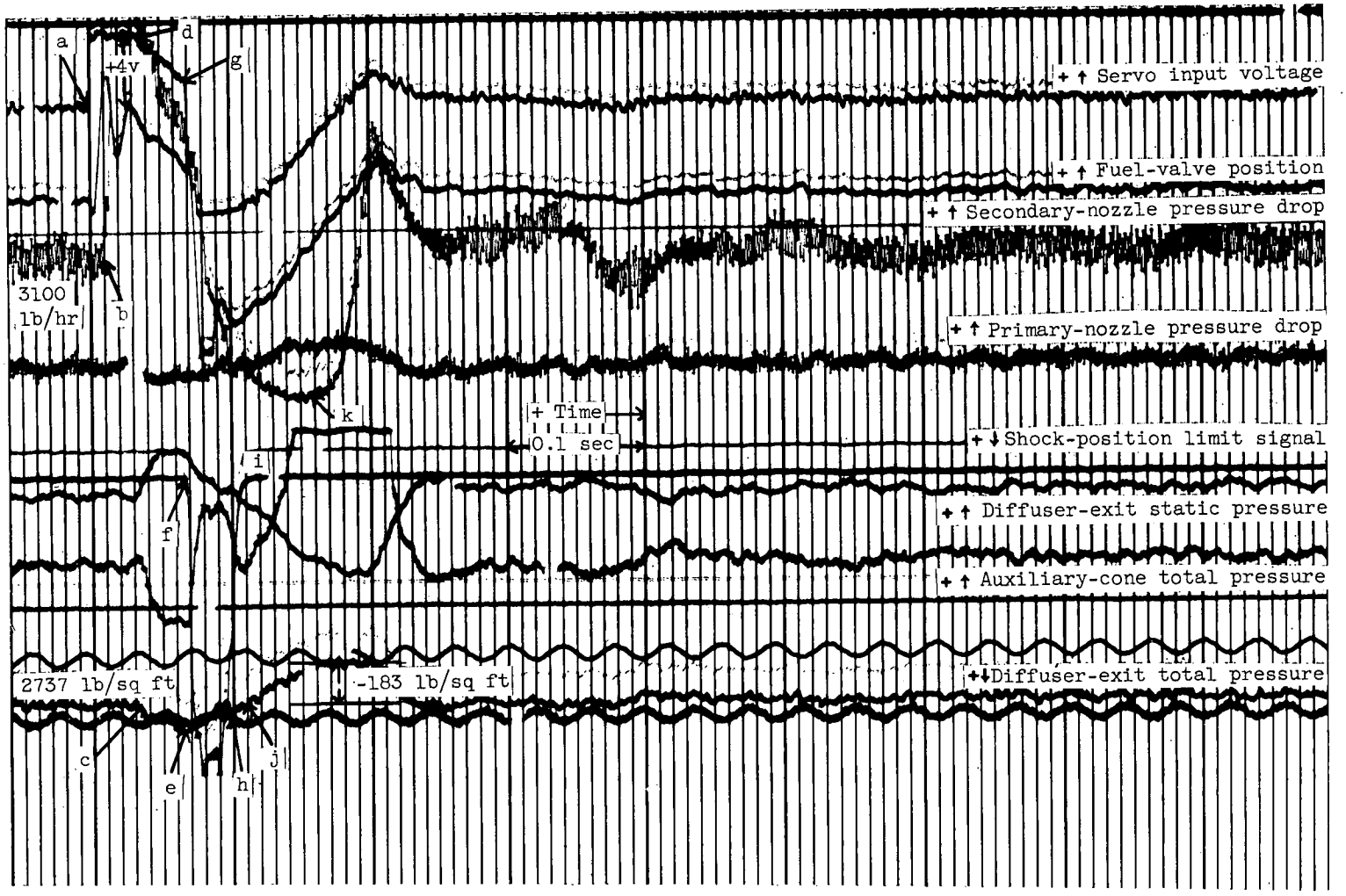

Figure 24. - Operation of shock-position limit in controlled system. Flight Mach number, 1.99; zero angle of attack; 0.85 P'_{ac} schedule; loop gain, 0.532; $1/\tau$, 20 sec^{-1}; free-stream static pressure, 439 pounds per square foot; step disturbance, +4 volts or +1112 pounds per hour.

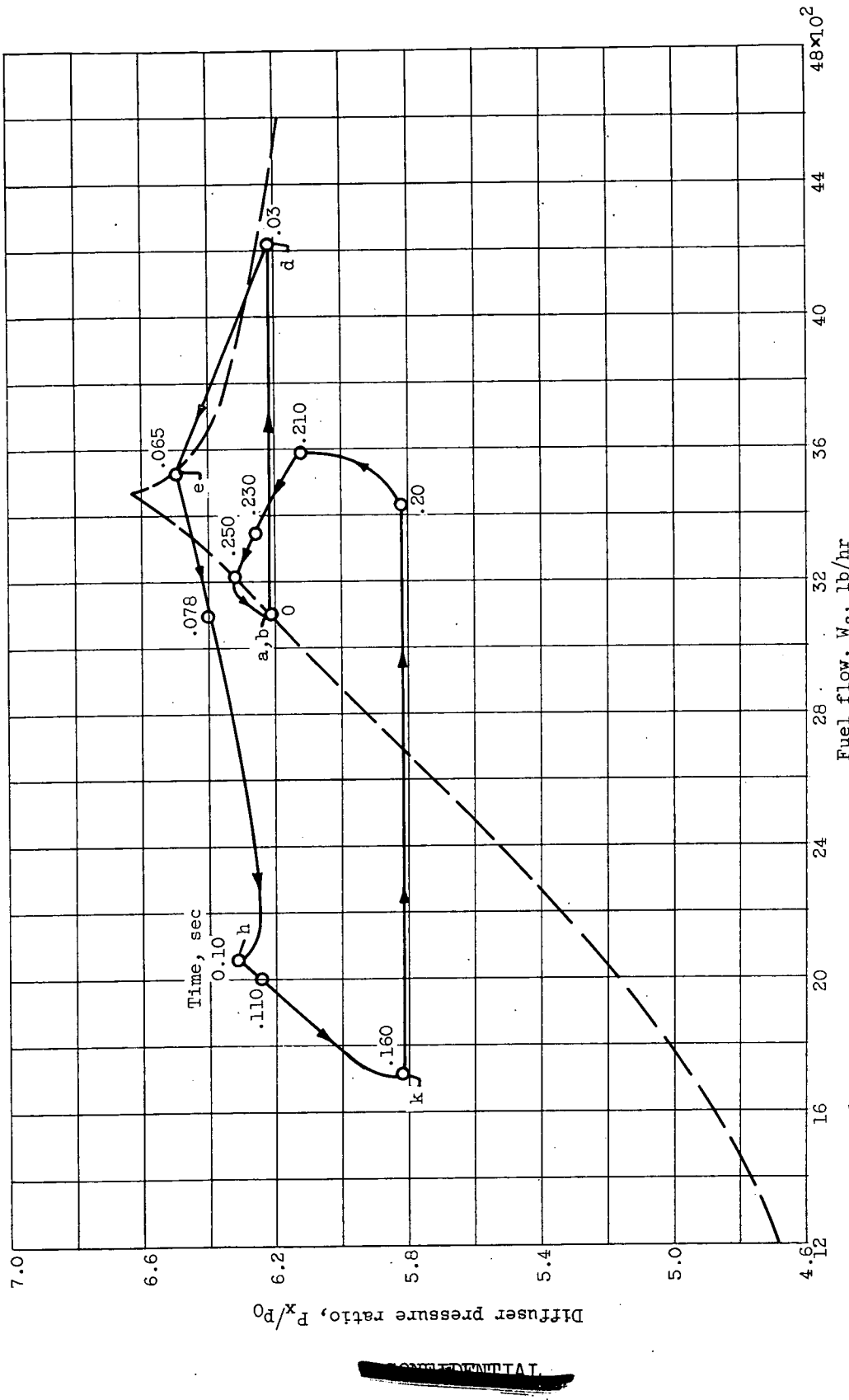

Figure 25. - Superposition of transient of figure 24 on diffuser performance map. Flight Mach number, 1.98; zero angle of attack; loop gain, 0.532; $1/\tau$, 50 sec^{-1}; step disturbance, +4 volts or +1112 pounds per hour.

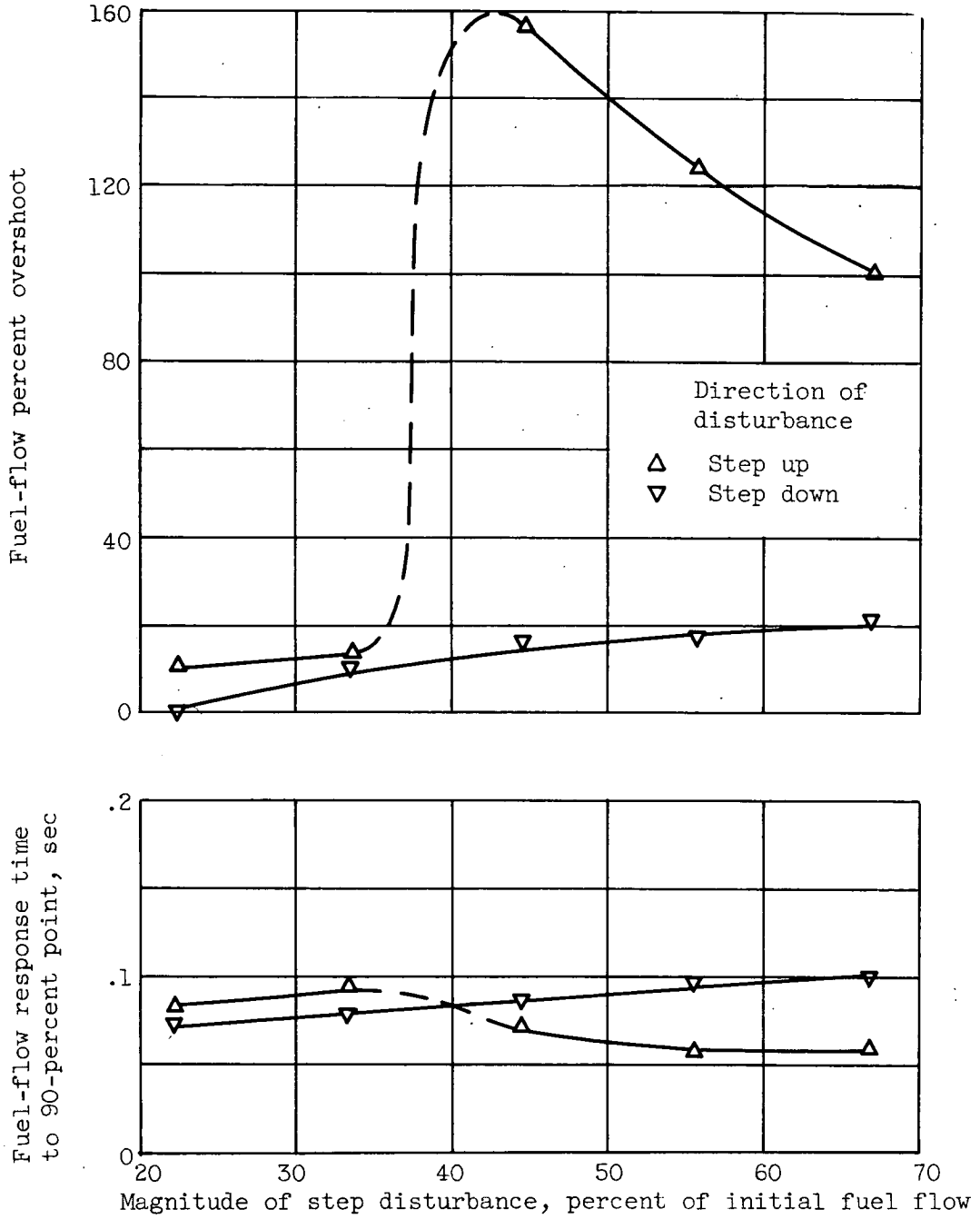

Figure 26. - Control-system response characteristic as a function of magnitude of disturbance with shock-position limit. Flight Mach number, 2.0; zero angle of attack; 0.85 P'_{ac} schedule; loop gain, 0.532; $1/\tau$, 50 sec^{-1}; initial fuel flow, 3100 pounds per hour.

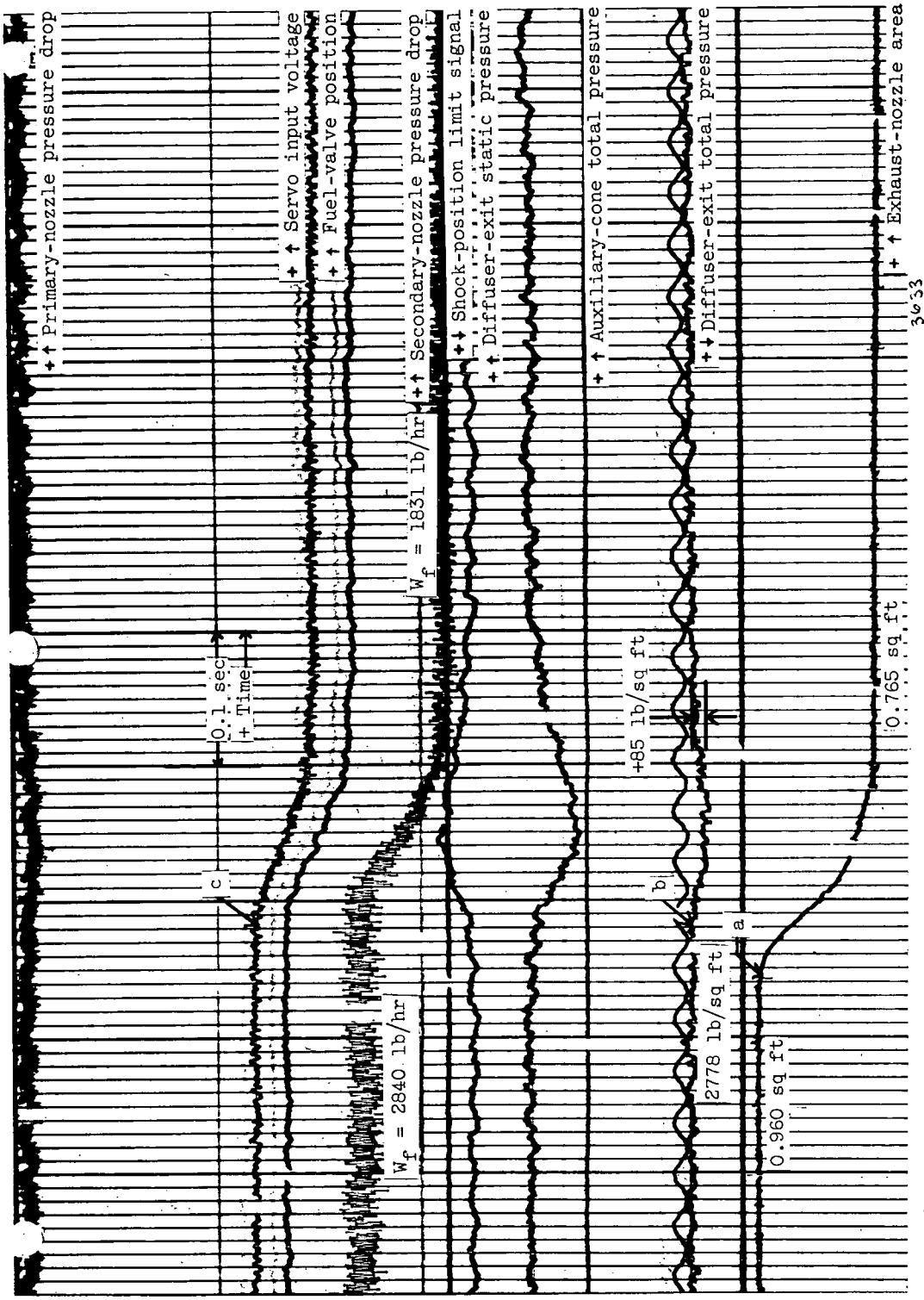

Figure 27. - Exhaust-nozzle-area transient. Flight Mach number, 1.99; zero angle of attack; 0.85 P'_{ac} schedule; free-stream static pressure, 440 pounds per square foot; loop gain, 0.532; $1/\tau$, 50 sec^{-1}.

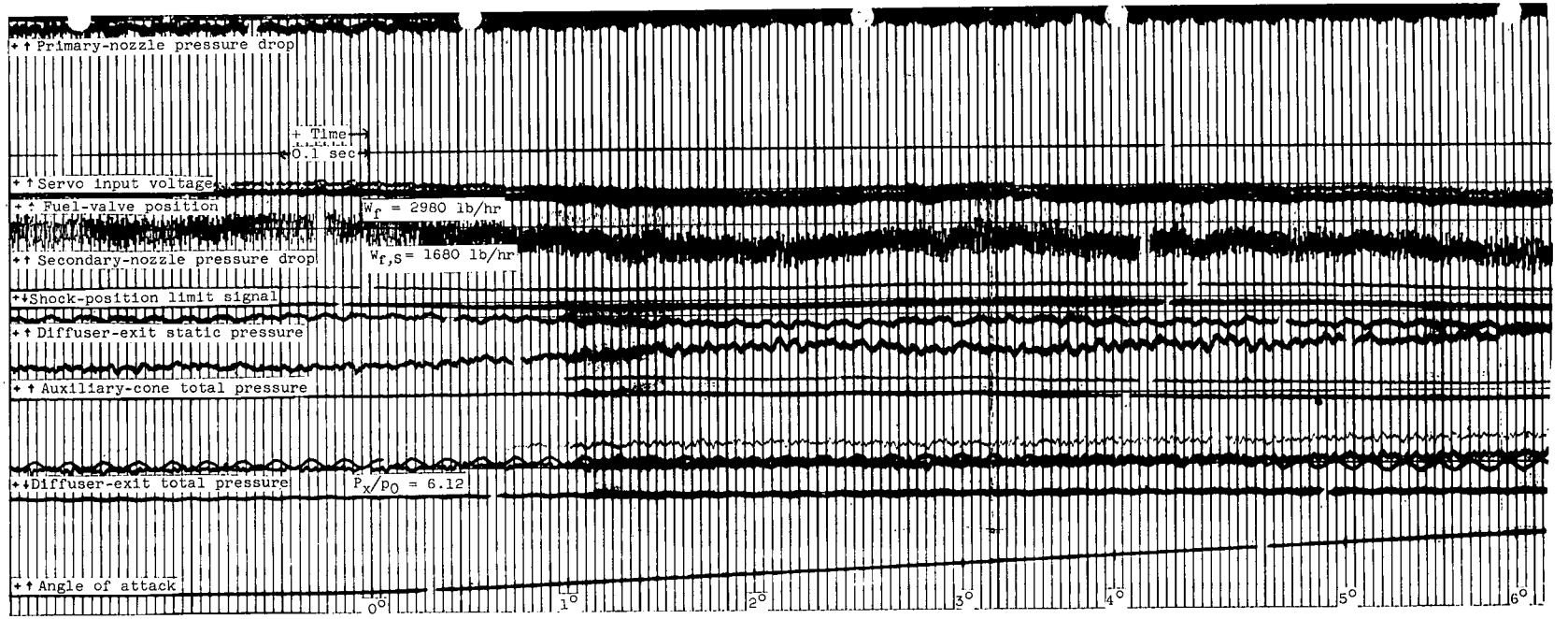

(a) Angle of attack, 0° to 6°.

Figure 28. - Angle-of-attack transient. Flight Mach number, 1.99; 0.85 P'_{ac} schedule; free-stream static pressure, 445 pounds per square foot; loop gain, 0.532; 1/4, 50 sec^{-1}.

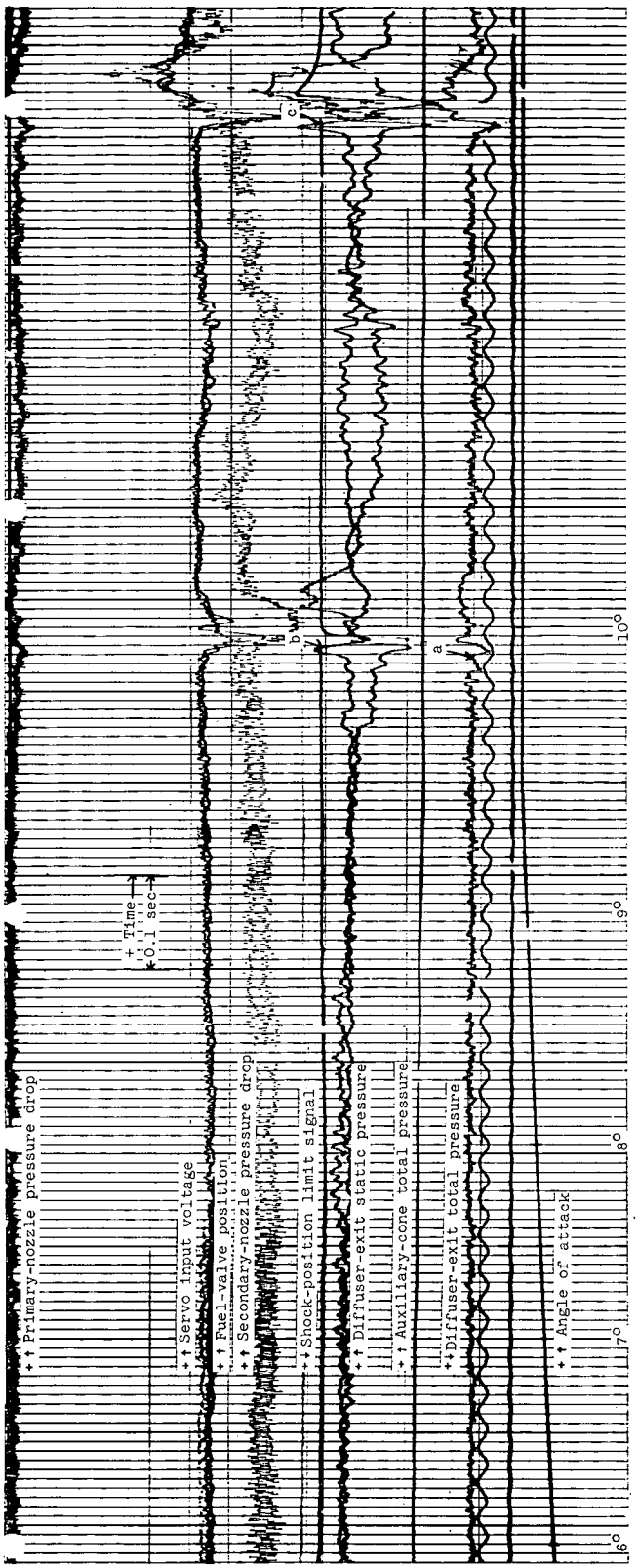

(b) Angle of attack, 6° to 10°.

Figure 28. - Concluded. Angle-of-attack transient. Flight Mach number, 1.99; 0.85 P'_{ac} schedule; free-stream static pressure, 445 pounds per square foot; loop gain, 0.532; 1/4, 50 sec^{-1}.

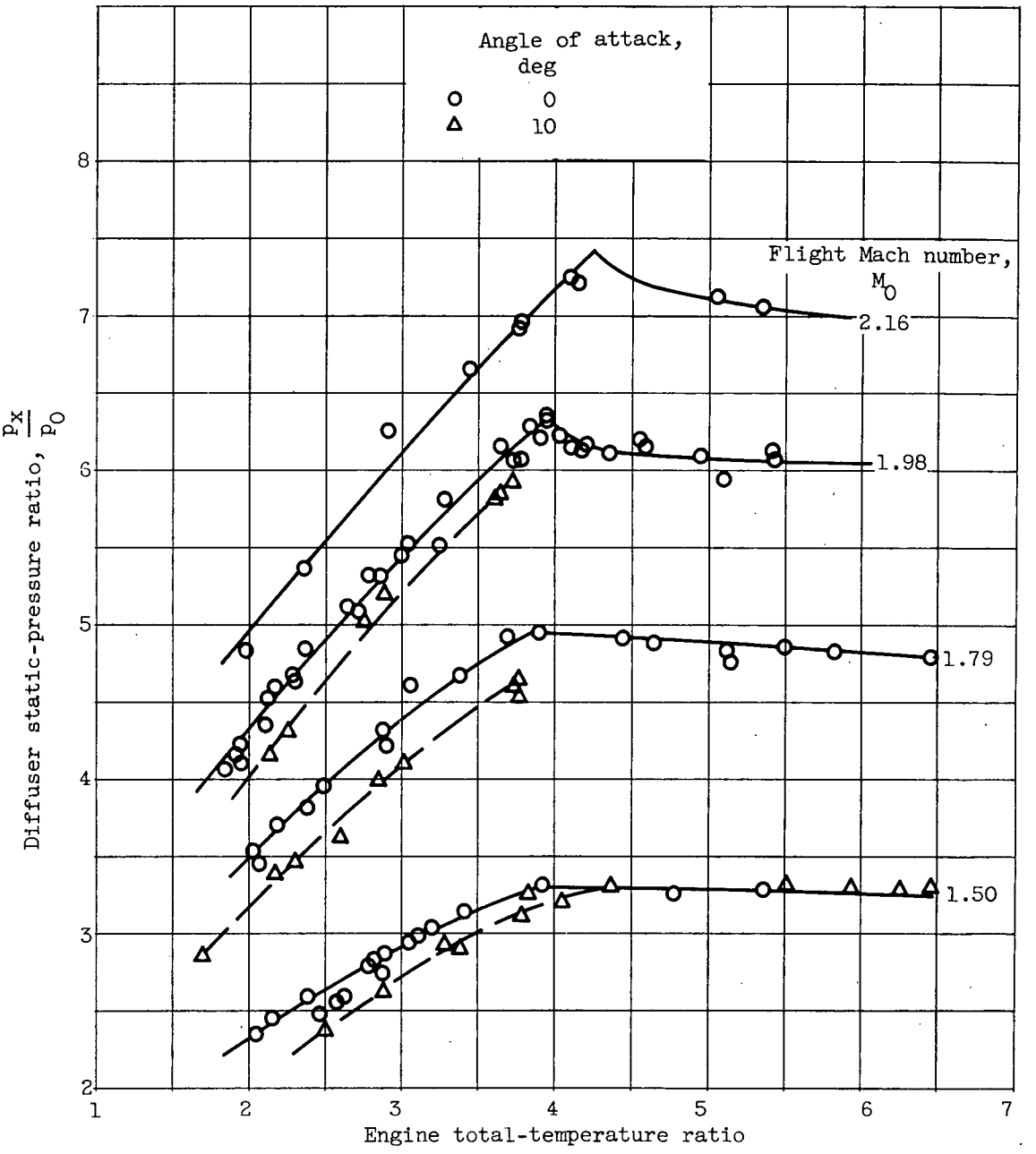

Figure 29. - Variation of diffuser static-pressure ratio with engine total-temperature ratio.

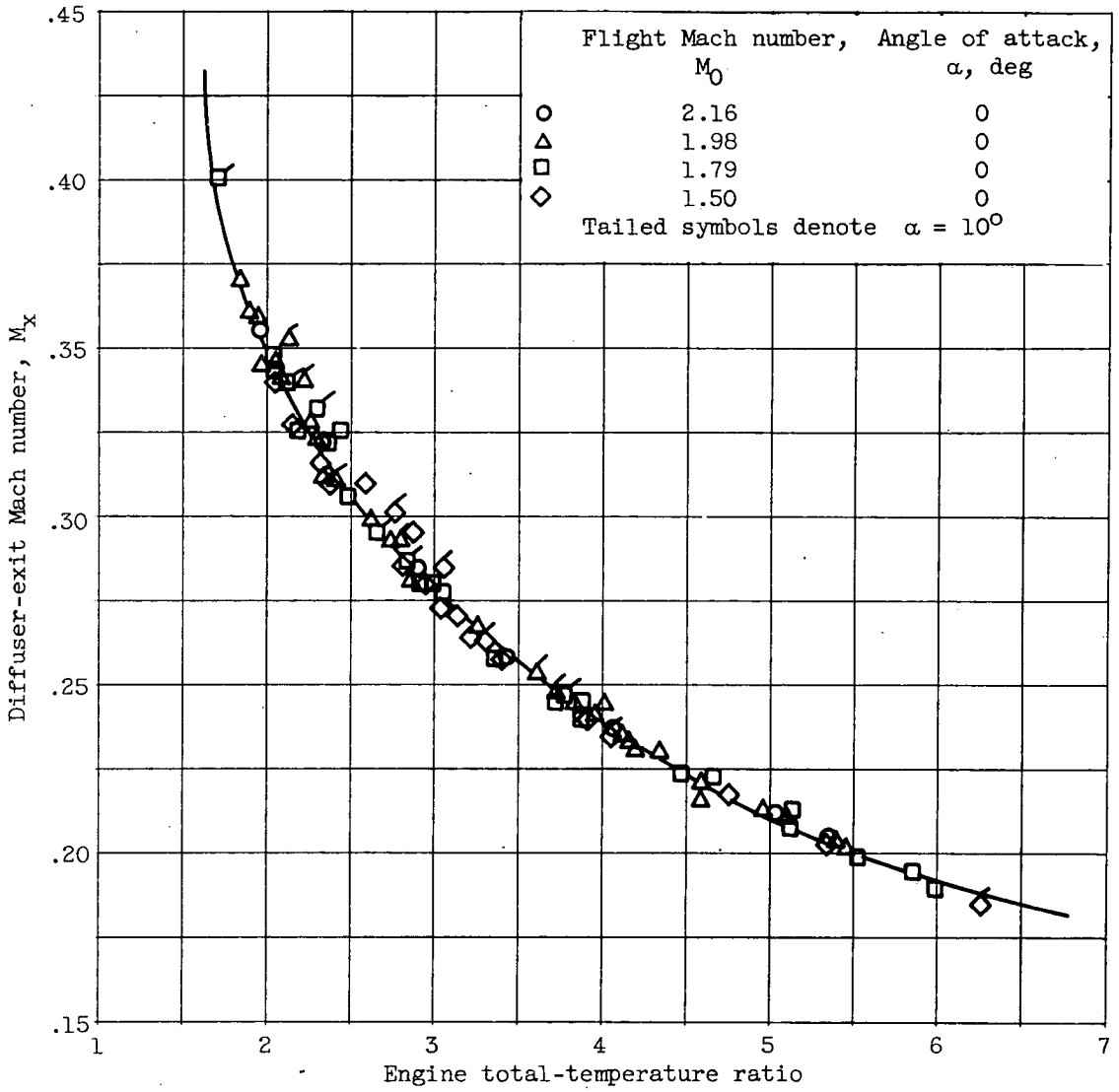

Figure 30. - Variation of diffuser-exit Mach number with engine total-temperature ratio.

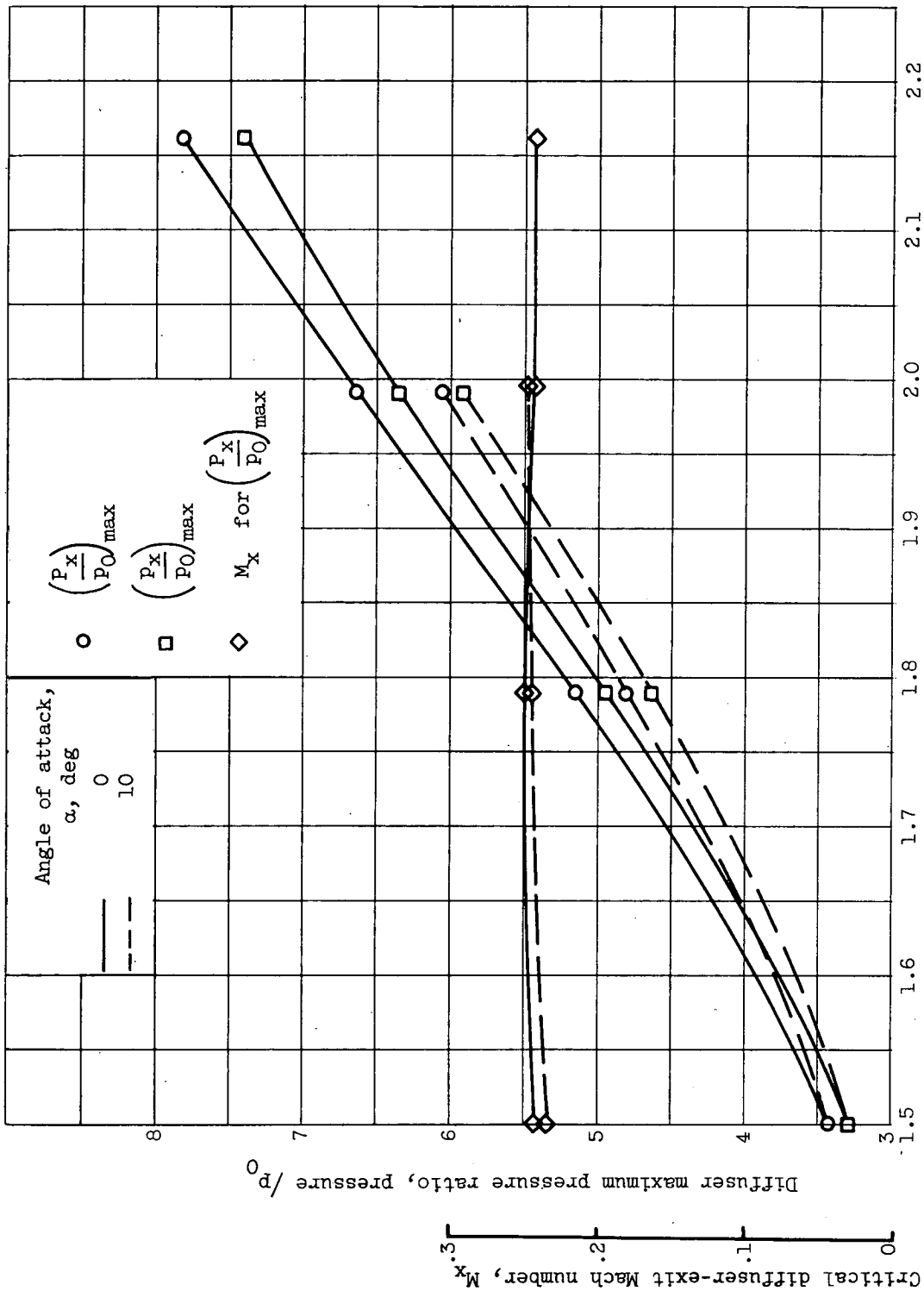

Figure 31. - Variation of control parameters with flight Mach number and angle of attack.

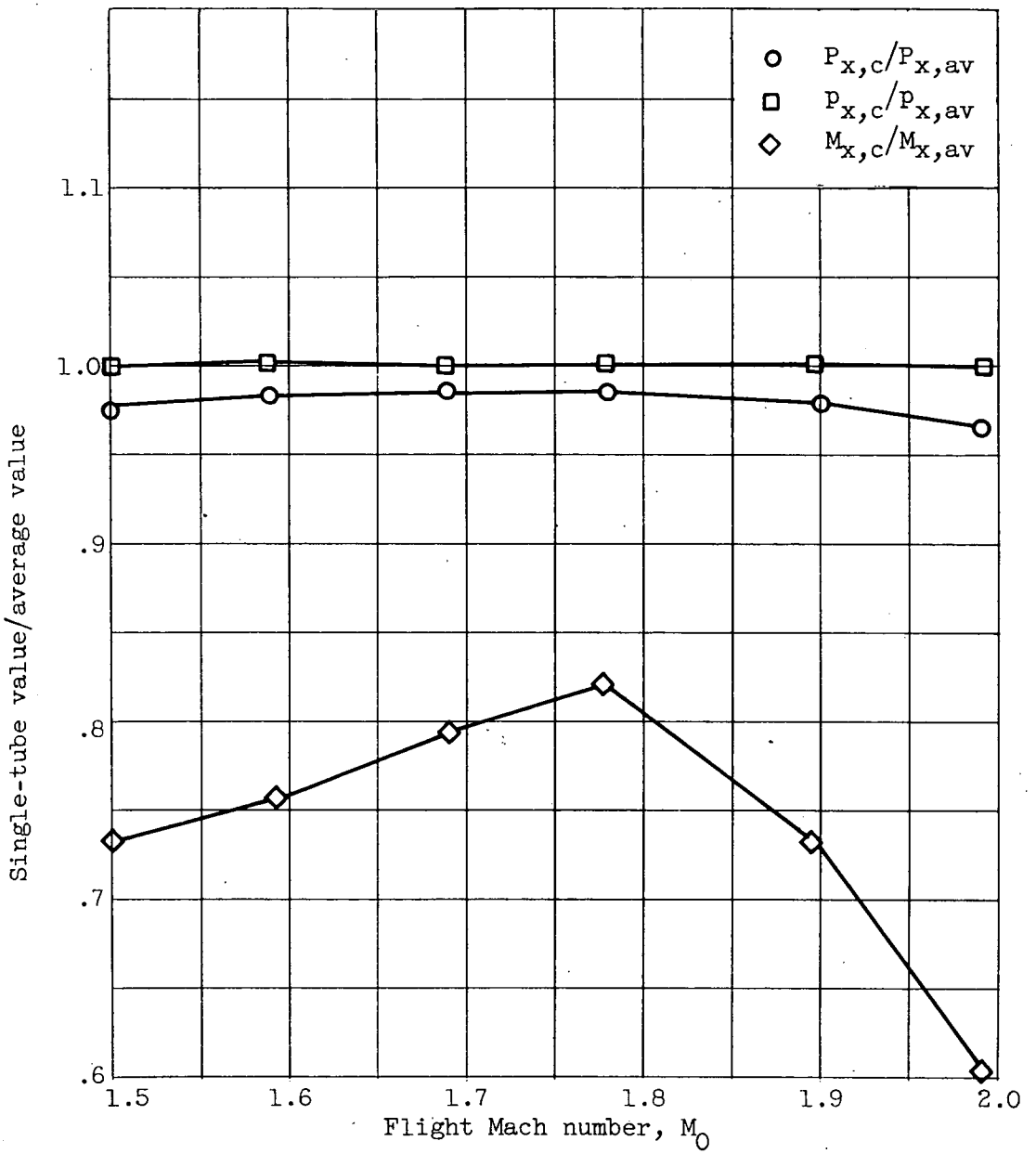

Figure 32. - Ratio of single-tube values to average values of control parameters during operation on 0.9 P'_{ac} schedule.

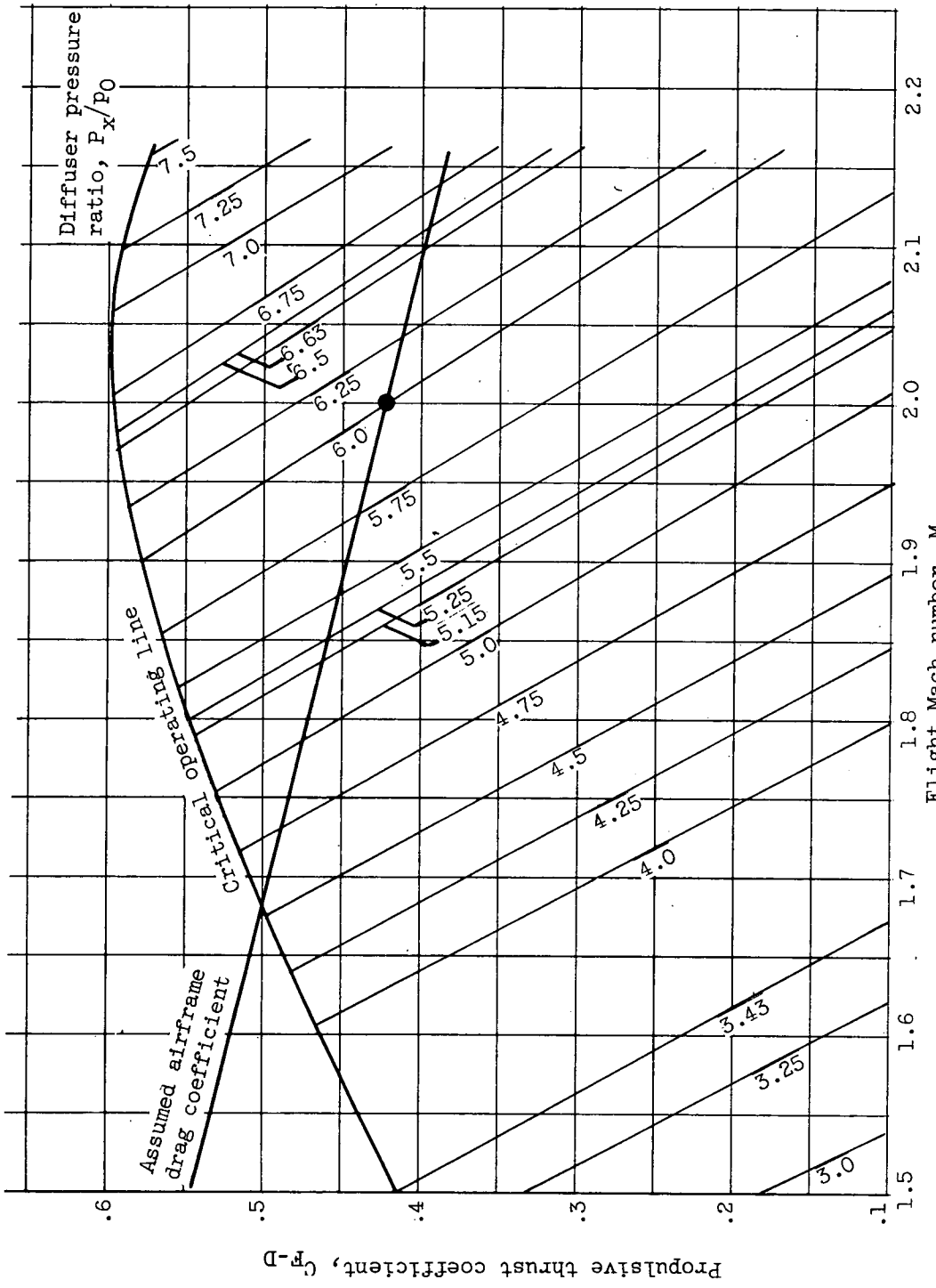

Figure 33. - Thrust coefficient at constant diffuser pressure ratio.

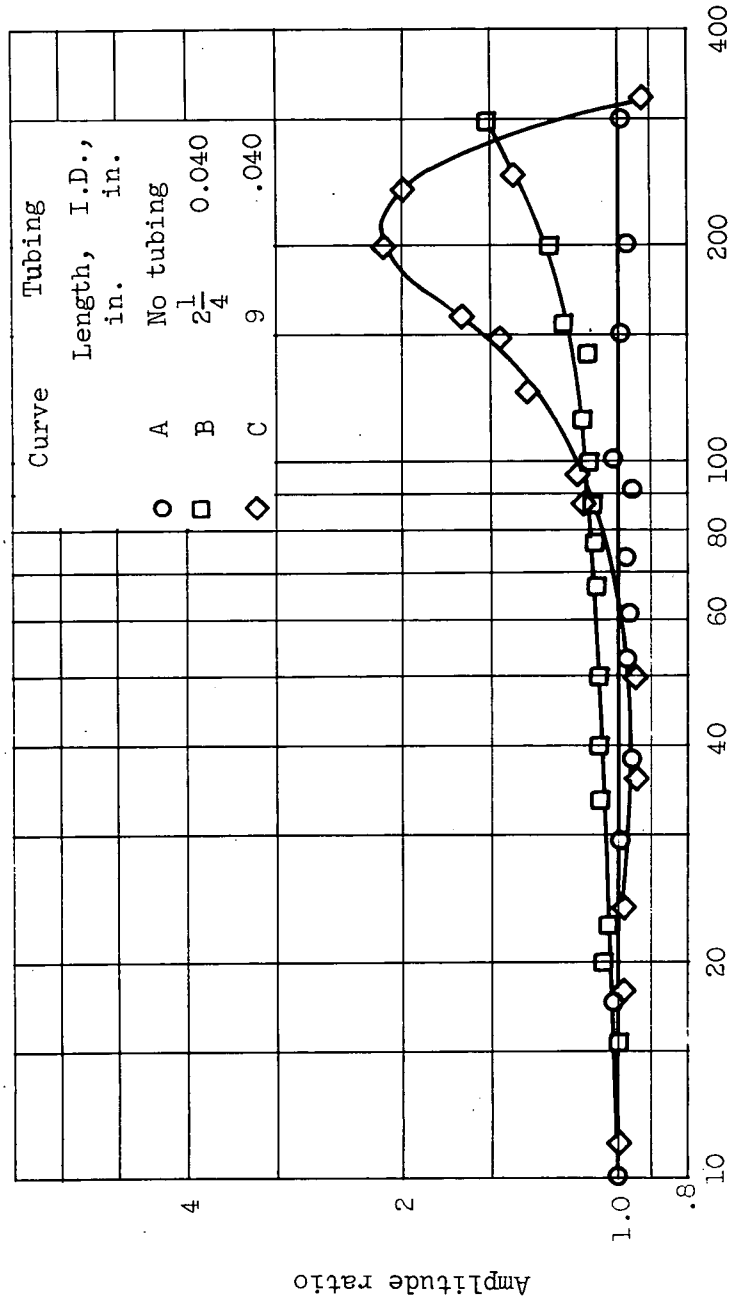

(a) Amplitude ratio.

Figure 34. - Frequency response characteristic for type I pressure transducer.

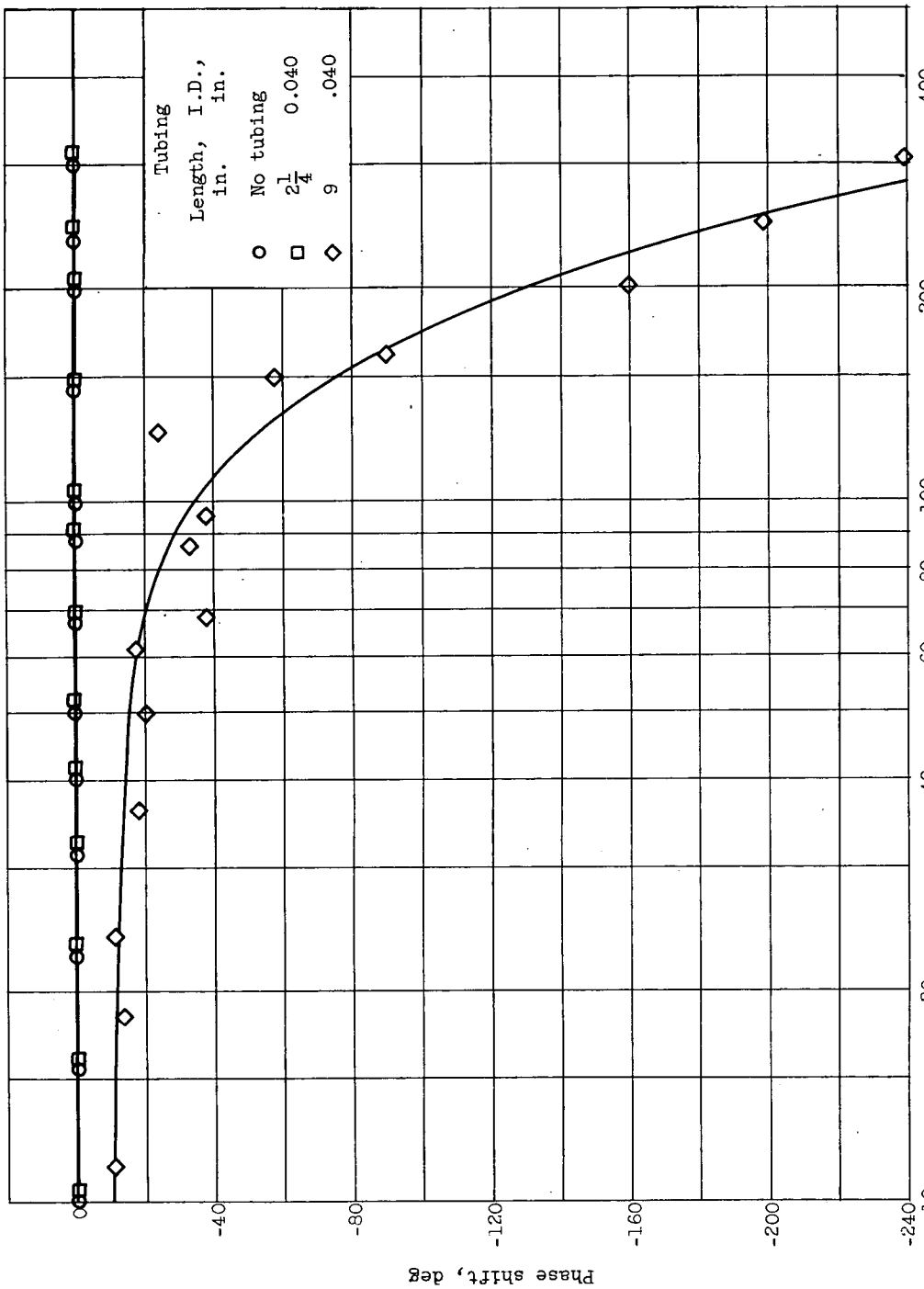

(b) Phase characteristic.

Figure 34. - Concluded. Frequency response characteristic for type I pressure transducer.

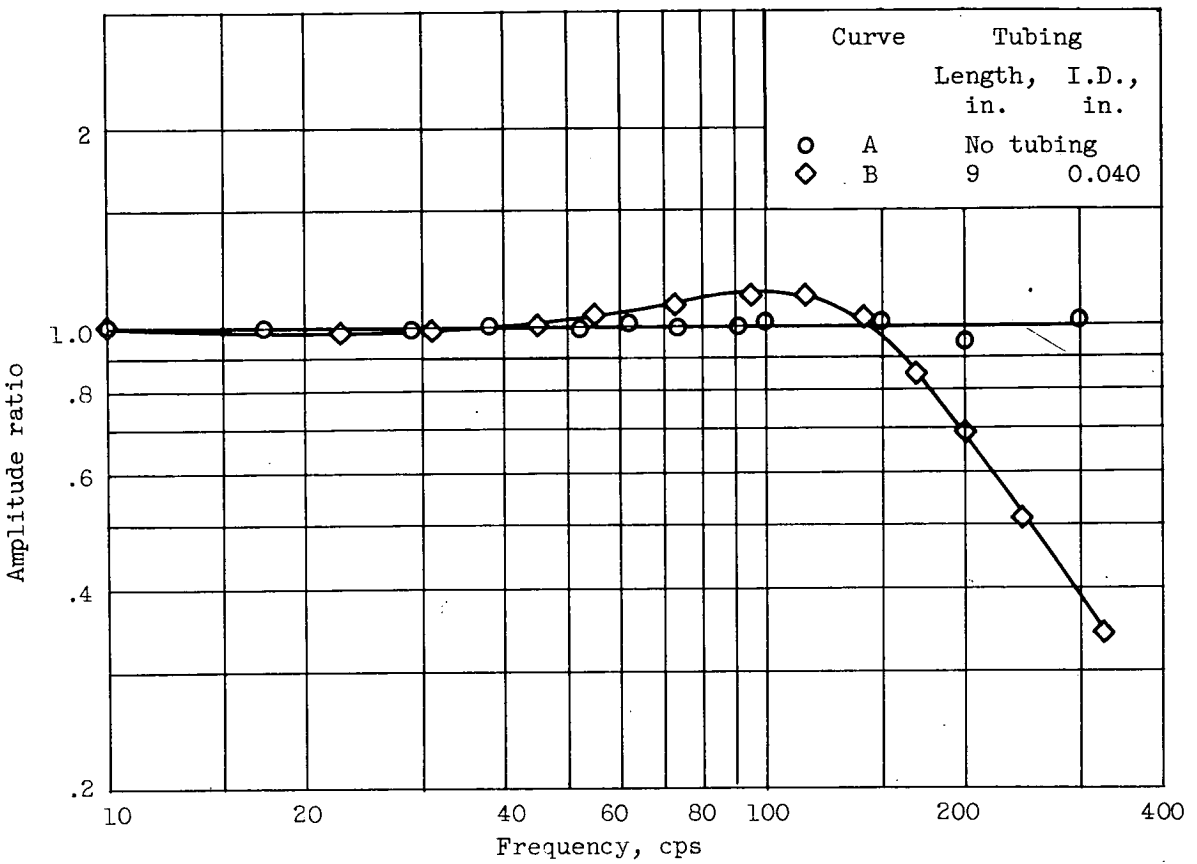

(a) Amplitude ratio.

Figure 35. - Frequency response characteristic for type II pressure transducer.

[redacted]

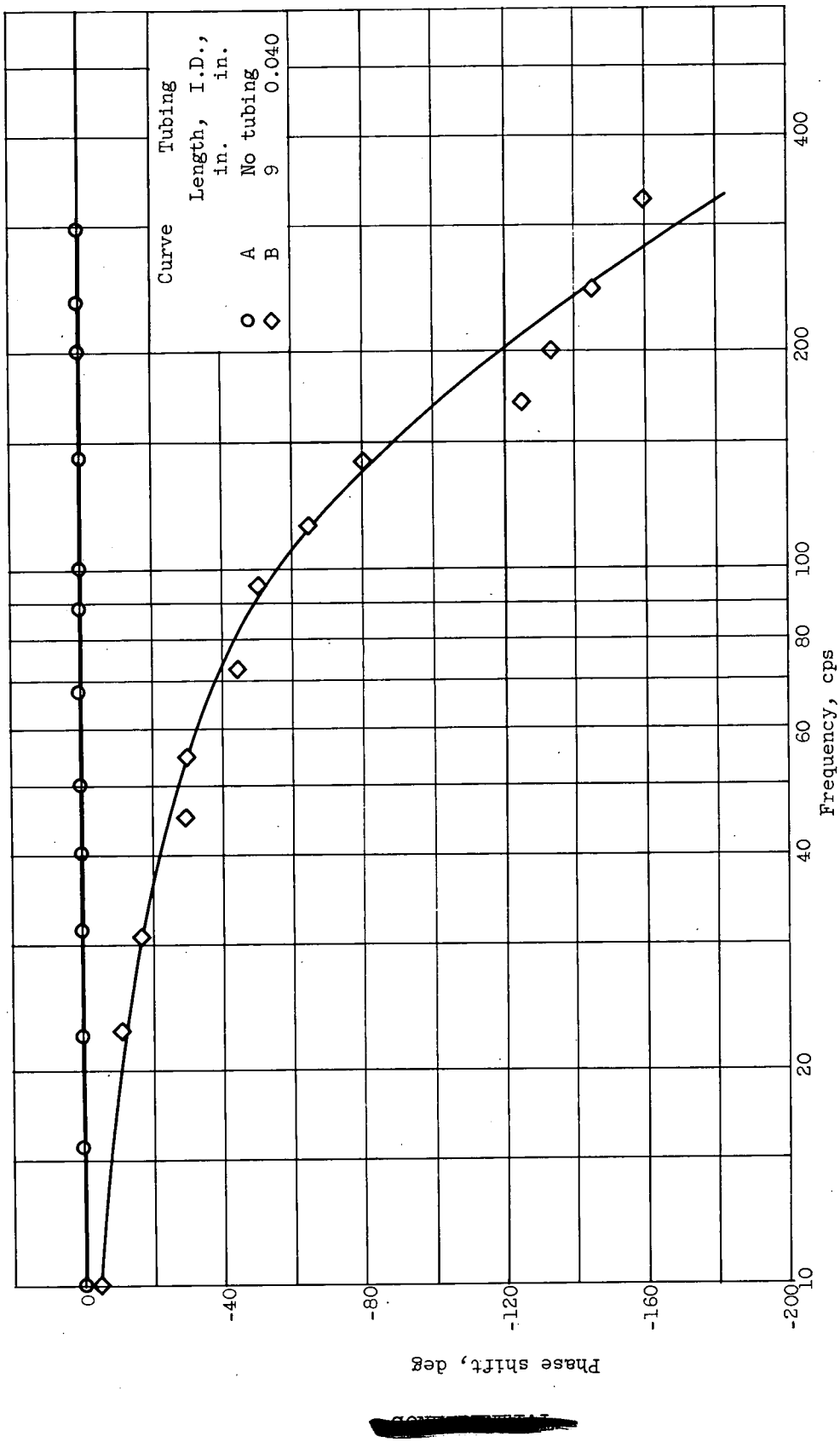

(b) Phase characteristic.

Figure 35. - Concluded. Frequency response characteristic for type II pressure transducer.

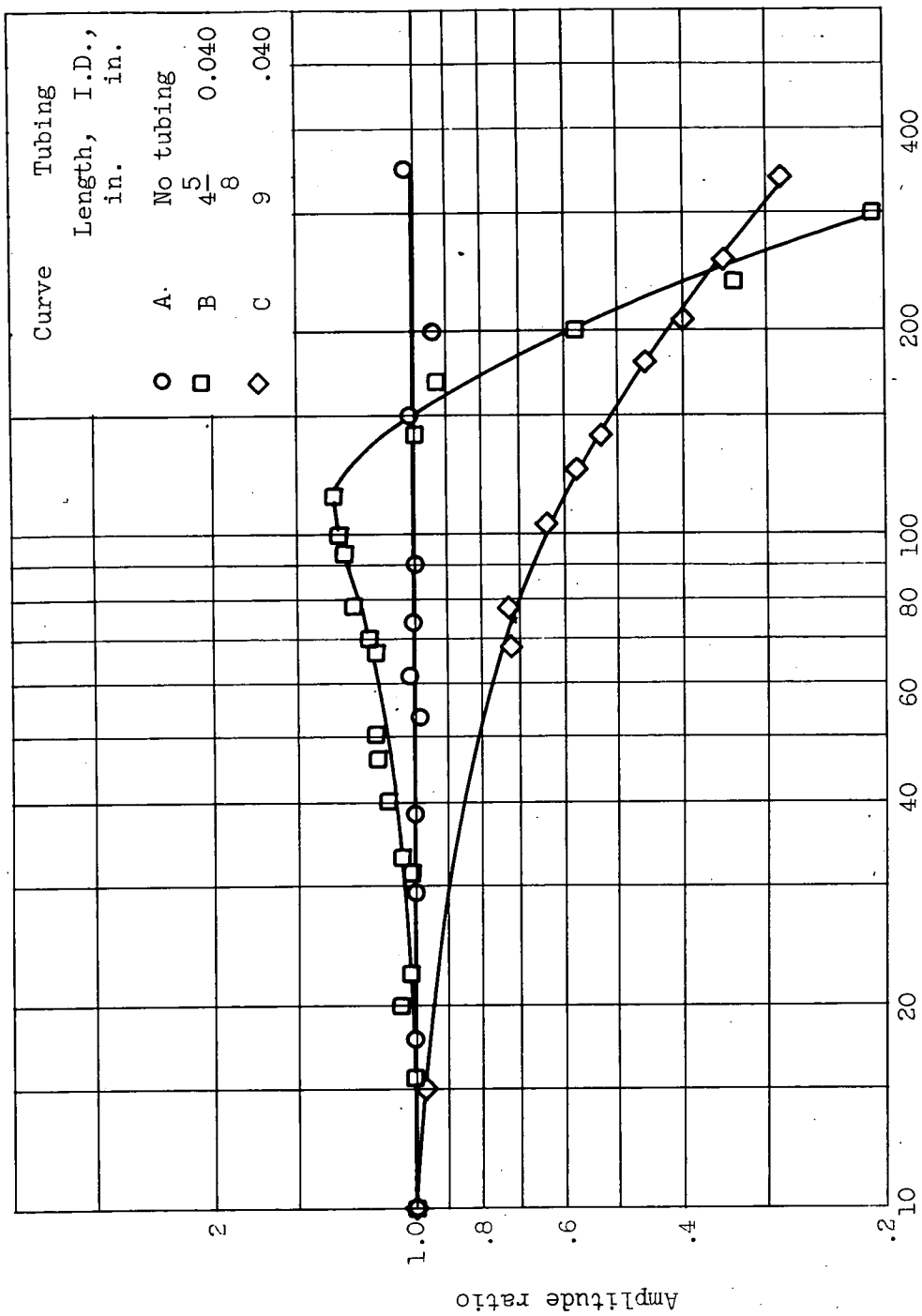

(a) Amplitude ratio.

Figure 36. - Frequency response characteristic for type III pressure transducer.

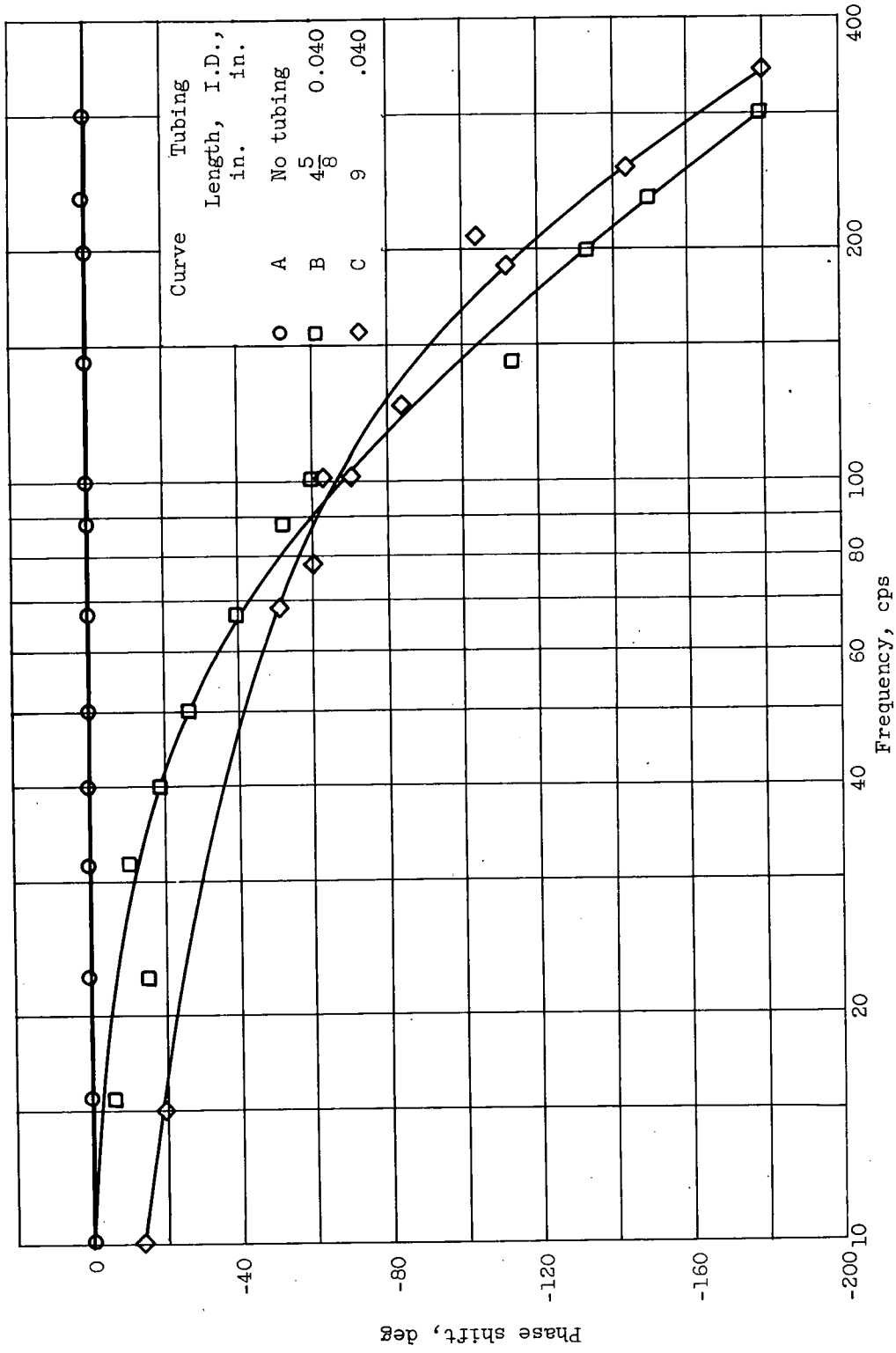

(b) Phase characteristic.

Figure 36. - Concluded. Frequency response characteristic for type III pressure transducer.